SKYTEM Airborne surveys worldwide

SkyTEM Survey:
British Columbia, Canada
Data report

Client: Geoscience BC

Date: October 2015

Reference: Geoscience BC Report 2016-03

SkyTEM Surveys ApS, Dyssen 2, 8200 Aarhus N, Denmark, +45 8620 2050

Contents

Introduction

In the period 11th of July to 22nd of August, 2015 a time domain electromagnetic and magnetic survey was performed by SkyTEM Surveys ApS in British Columbia, Canada. The survey area is presented on Figure 1. The survey, requested by Geoscience BC, consists of 20,999 line km, with 20,337 km in the Peace block (incl. NE extension and HRFN infill), 425 km in the DOIG block and 237 km in the Charlie Lake block. The following report describes the data acquisition, and processing of the survey data.

This report does not include any geological interpretations of the geophysical dataset.

SkyTEM has agreed to deliver SkyTEM standard processed electromagnetic data together with processed magnetic data. Please note, that this does not include manually culling of data due to galvanic or capacitive coupling.

Basic survey information and key personnel are listed in Table 1.

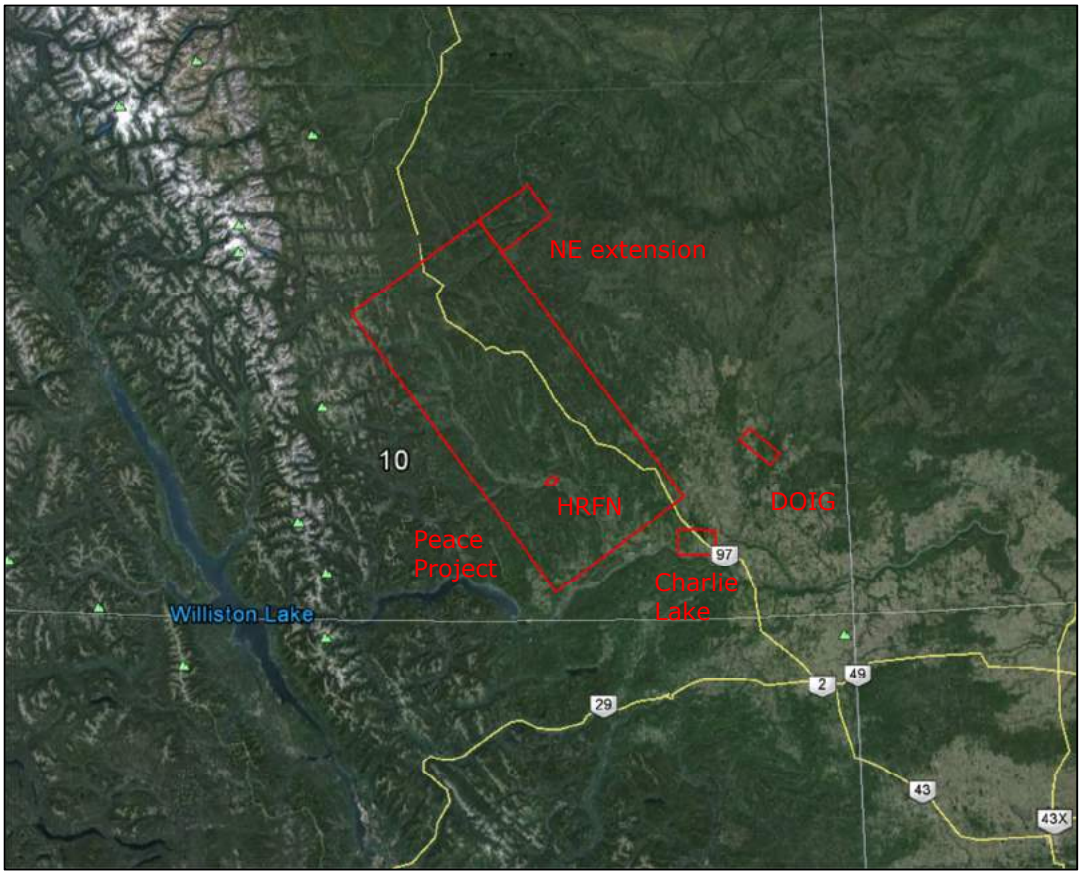

Figure 1 Survey location overview. Survey area is indicated by the red polygons.

Client		Geoscience BC
Client representative		Mr Carlos Sales
Contact Person at SkyTEM		Mr Bill Brown Email: bb@skytem.com
SkyTEM project manager		Ms Anne Have Rasmussen Email: ahr@skytem.com
Field crew		Mr Jean-Christophe Richard Mr Jason Marcil Mr Eric Rooen
Field work		11th of July to 22nd of August, 2015
Flight operation	Helicopter type Pilot Average flight speed Nominal flight height	Eurocopter Astar 350 B3, operated by Bailey Helicopters Ltd Mr Keith Varga Mr Erwin Karrer 118.5 kph 30 m
Report	Data processing and presentation QC by	Ms. Anne Have Rasmussen Ms Sara Thofte Mr Per Gisselø

Table 1 Basic personnel and survey information.

Definition of the areas

The survey is comprised of one main block (Peace) and three additional areas (DOIG, NE extension and Charlie Lake); Figure 2 gives an overview of the planned flight lines. The projection in the report and data delivery folders has been kept in UTM Zone 10N (WGS84).

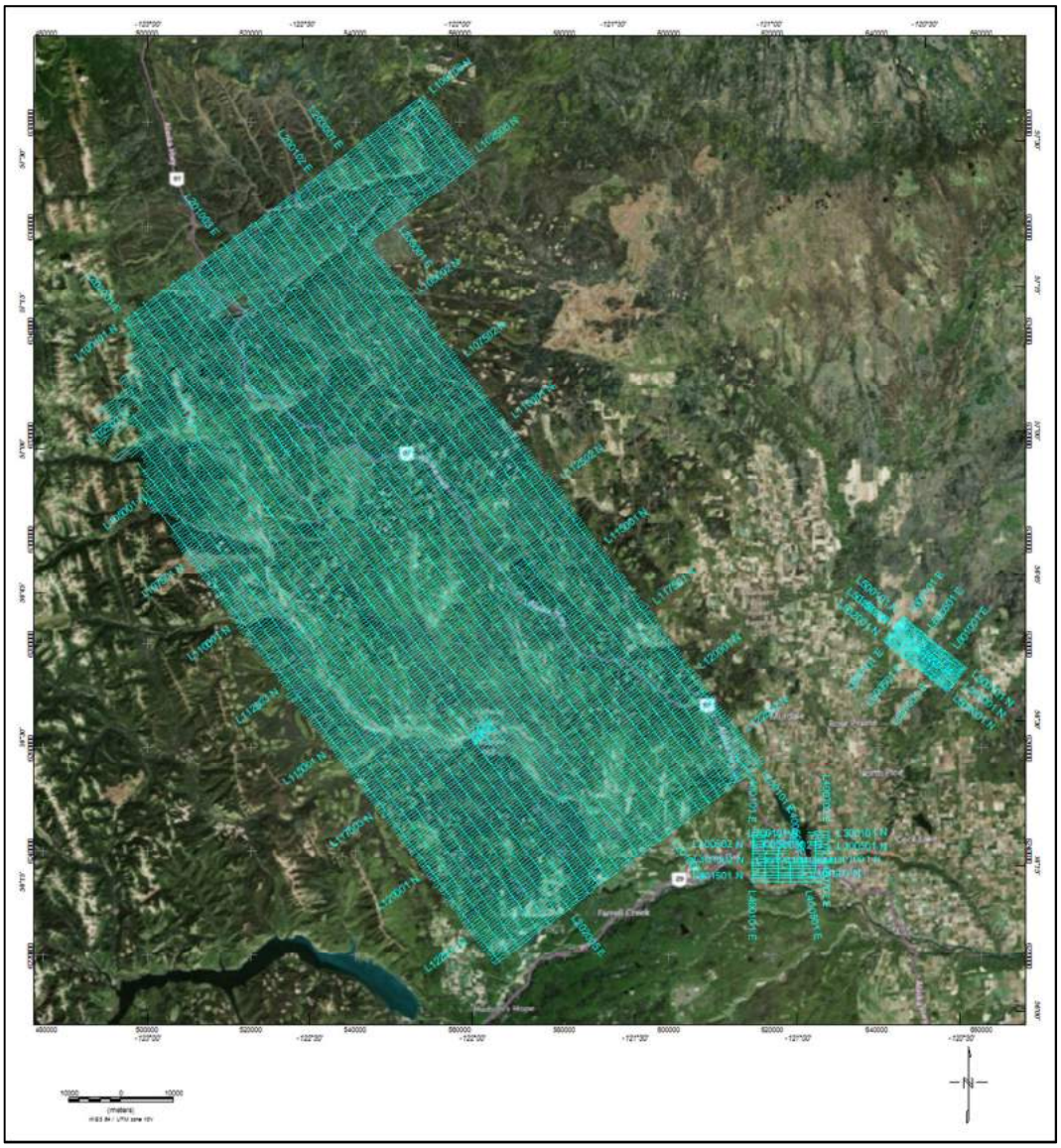

Figure 2 Flight lines marked with blue. UTM Zone 10N (WGS84).

Instruments and parameter setup

The instrumentation consists of a time domain electromagnetic system including a data acquisition system, two inclinometers, two altimeters, two DGPS', a magnetometer and a magnetic data acquisition system.

The equipment setup has been chosen as a dual moment configuration with a Low moment (LM) with a peak moment of ~ 3,000 NIA and a High Moment (HM) with a peak moment of ~ 490,000 NIA.

A dual moment system provides a major advantage over single moment systems in that it is possible to measure a wider range of time gates. In LM mode early time gates can be measured allowing more accurately resolution in the near surface while in the HM mode, deep penetration can be achieved.

A simplified illustration of the SkyTEM system can be seen in Figure 3 which displays the approximate location of instruments that are rigidly attached to the frame. A similar configuration was used for this survey.

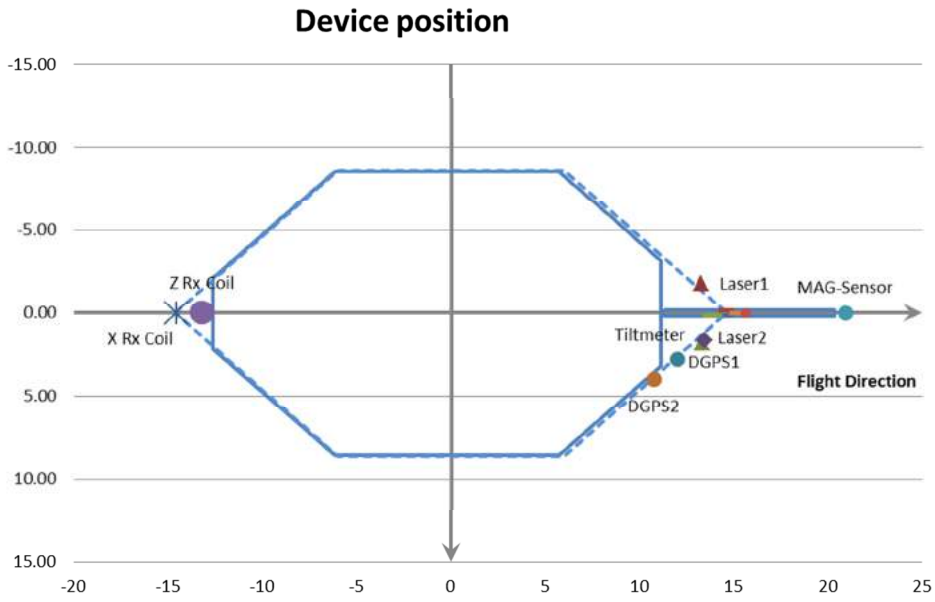

Figure 3 Sketch showing the frame and the position of the basic instruments. The blue line defines the transmitter loop. The horizontal plane is defined by (x,y).

The x and y axis define the horizontal plane. The z axis is perpendicular to (x,y). X is positive in the flight direction, y is positive to the right of the flight direction, and z is positive downwards.

Three DGPS systems are mounted on a boom located towards the front of the frame. Data from two DGPS receivers are recorded by the EM data acquisition system while a

third DGPS is recorded by the magnetic data acquisition system. The DGPS systems are used for time stamping, positioning, and correlation of the EM and magnetic datasets.

The generator used to power the transmitter is suspended ~20 m below the helicopter.

A more thorough description of the individual instruments can be found in Appendix 1.

Synchronizing the data

All recorded data are marked with a time stamp used to link the different data types. The time stamp is in UTC/GMT.

The time stamp formats are either

- Date and Time defined as; yyyy/mm/dd hh:mm:ss.sss
  or
- Datetime values defined as the number of days since 1900-01-01 and seconds of the day; ddddd.sssssssss

Waveform of the TEM system

The complete TEM equipment has been tested at the Danish National Reference Site. Appendix 3 provides a description of the waveform modelling of the SkyTEM system.

If third party processing or inversions are undertaken using the processed data as the base dataset (i.e. .gdb EM data) the calibrated gate center times in Appendix 2 should be used.

The waveforms for Low moment and High Moment are shown in Appendix 3.

Data acquisition

Planned flight lines covering the full survey are shown in Figure 2. An overview of flown versus planned lines can be seen on Figure 4. The surveyed flight path (what was actually flown) can be seen as red lines imposed on planned flight lines. Discrepancies are seen from the planned lines where cultural features such as roads, buildings, and antennas necessitate a diversion.

The nominal terrain clearance is ~50 m, with an increase over forests, power lines, or any other obstacles or hazards. The safe flying height during survey is always based on the pilot's assessment of risk and deviations from nominal values are at the discretion of the pilot.

The helicopter airspeed was set not to exceed 150 kph with an average of 120 – 150 kph for a flat topography with no wind. This may vary in areas of rugged terrain and/or windy conditions.

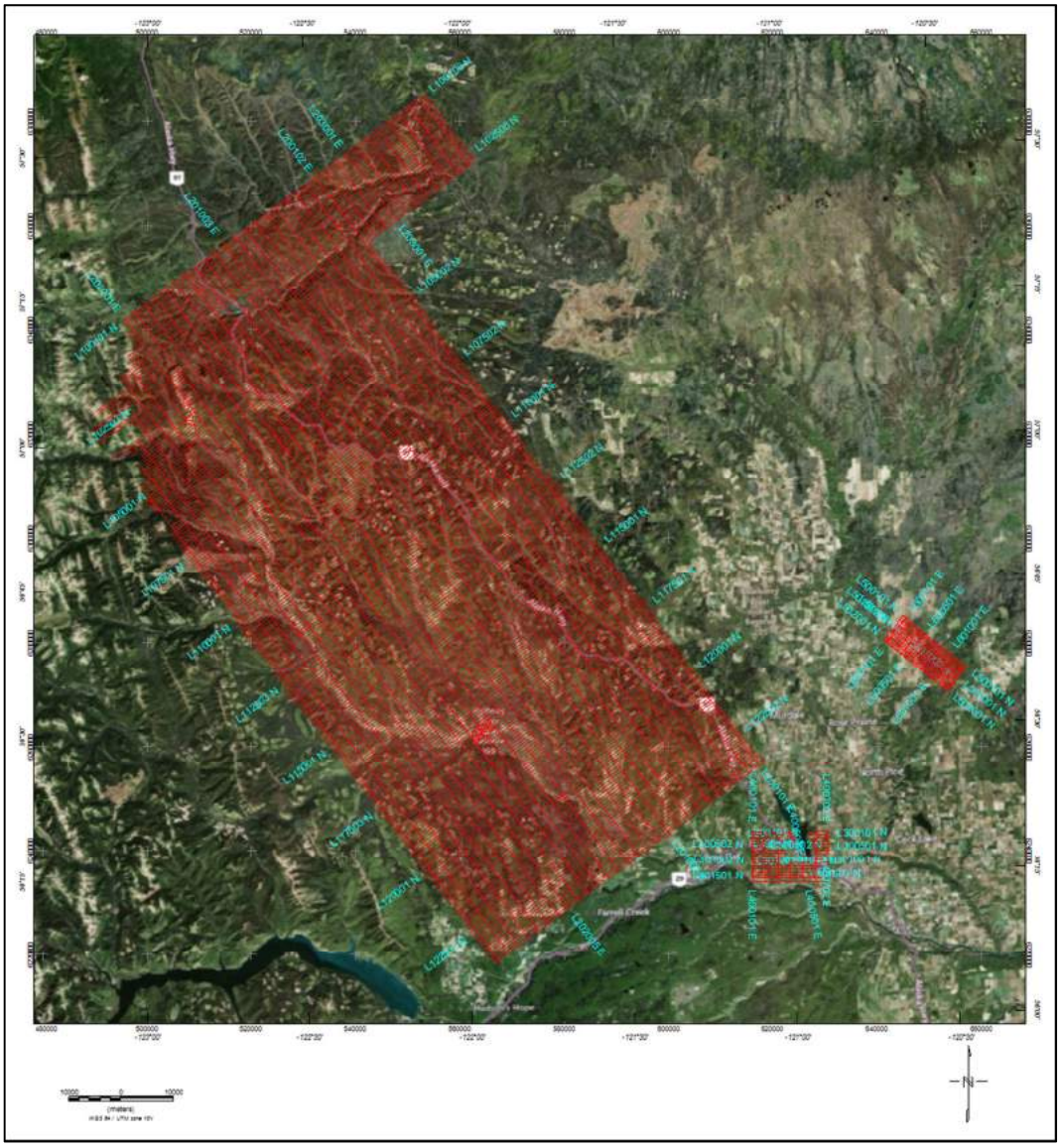

Figure 4 Flown lines (red) superimposed on planned lines (blue) for the survey in Peace Project, UTM Zone 10N (WGS84)

Ground Base Stations

The DGPS and magnetic base stations were positioned at the closest accessible place to the survey areas.

DGPS base station

Effort was made to ensure that the DGPS base station was placed at a location of maximum possible view to satellites and out of any metallic objects that could influence the GPS antenna.

Table showing DGPS base station location (Lat/Lon (WGS84)):

Area	Lat	Lon	Ell. Height
Landing 1	56 29 15.09444	-121 11 48.91577	825 masl
Landing 2	56 29 15.51065	-121 11 45.15523	816 masl
Landing 3	57 09 47.19693	-122 40 10.52400	1236 masl

Magnetometer base station

Effort was made to ensure that the base station magnetometer was placed in a location of low magnetic gradient, away from electrical transmission lines and moving metallic objects, such as motor vehicles and aircraft.

The table below shows the location of the magnetic base station (Lat/Lon, (WGS84)):

Magnetometer Base station	Lat	Lon	Height
Landing 1	56.487469	-121.196757	833 masl
Landing 2	56.733921	-121.849297	941 masl
Landing 3	57.16327	-122.66943	1249 masl

Flight reports

For each flight, a report with key information regarding the data acquisition is made in the field. Listed in the reports are details on the weather, specials data parameters and other events which may influence the data. Selected information from the flight reports can be seen in appendix 5.

Processed data

EM processing

In the following the processing performed by SkyTEM Surveys is presented.

All data are resampled to 10 Hz using the SkyTEM in-house software SkyLab.

The data are normalized in respect to effective Rx coil area, Tx coil area, number of turns and current giving the unit: $pV/(m^4 \cdot A)$.

The raw EM data are filtered using a filter with varying weights depending on signal level.

All auxiliary devices (DGPS, Laser altimeters, inclinometers) are moved to the center of the frame.

The final processed data are transferred into Oasis Montaj Geosoft Array channels (See table on the page below).

Tilt processing

The X and Y angle processing involves manual and automated routines using a combination of the SkyTEM in-house software SkyLAB and Oasis Montaj Geosoft.
The processing involves the following steps:

1. 3 sec box filter (SkyLAB)
2. Low pass filtering of 3.0 sec. (Geosoft)

Height processing

The height processing involves manual and automated routines using a combination of the SkyTEM in-house software SkyLab and Oasis Montaj Geosoft.
The processing involves the following steps:

1. Keeping the 5 highest values pr. second and discarding the rest to correct for the canopy effect (treetop filter)
2. 3 sec running box filter (smoothing filter)
3. Tilt correction
4. Averaging of the two laser values
5. Additional filters in Geosoft including:
    a. Low pass filter of 3.0 sec

DGPS processing

The DGPS has been processed using the Waypoint GrafNav Lite Differential GPS processing tool. The standard airborne settings have been used.

1. Import of base station (Master)
2. Import of airborne files (Rover)
3. Calculation of forward and reverse DGPS solution
4. Export as .txt file

The DGPS.txt files are used as input to the SkyLab software assuring DGPS corrected data in the processed files.

The ground speed, altitude, latitude and longitude from the processed DGPS are merged into the final GDB. Afterwards the coordinates are transformed into UTM Zone 10N (WGS84).

A low pass filter of 3.0 sec has been applied to the above mentioned parameters.

Digital elevation model

A digital elevation model (DEM) channel has been calculated by subtracting the filtered laser altimeter data from the DGPS elevation.

The processing to the final DEM involves the following steps:

1. Filtering and processing of the laser altimeter height as described above
2. DEM data received by subtraction of final filtered laser data from final processed DGPS altitude data
3. Grids produced using the minimum curvature method

The DEM of Peace Project is seen on

Figure 5, Geosoft DEM map and grid are included in the digital data delivery catalogue.

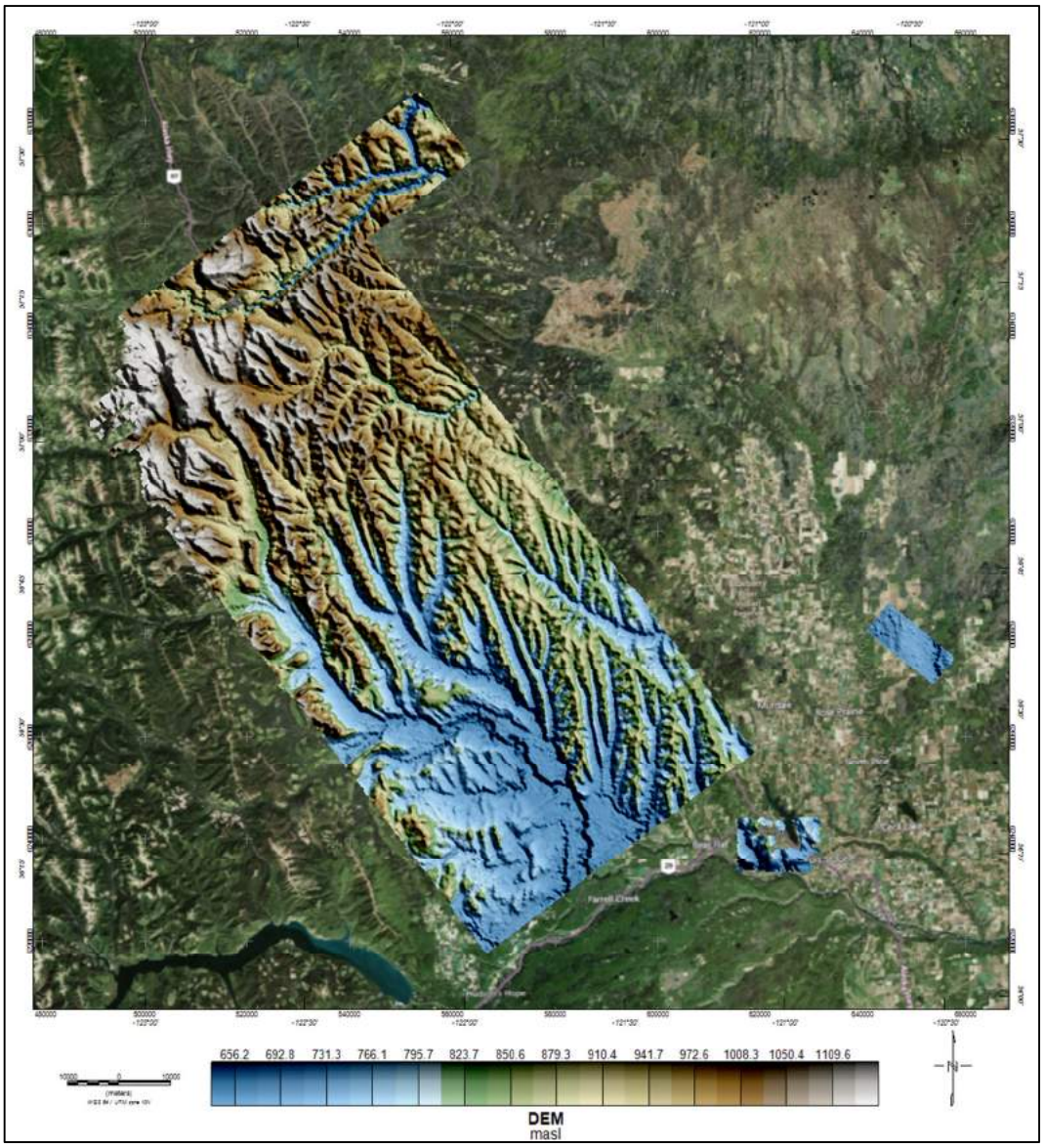

Figure 5 Digital Elevation Model (DEM) for Peace Project in meter above sea level. UTM Zone 10N *(WGS84).*

PLNI (Power Line Noise Intensity) monitor

The PLNI monitor values are derived from a frequency analysis of the raw Z-component EM data. For every low moment EM data block a PLNI value is obtained by Fourier transformation of the measured values for the latest low moment gate. The Fourier transformation is evaluated at the local power transmission frequency yielding the amplitude spectral density of the power line noise.

CAUTION - When evaluating the PLNI values one should be aware of the following factors that may give rise to anomalous PLNI patterns unrelated to the actual power line noise level:

- The low moment EM data are measured at a rate lower than the Nyquist criterion for the applied system bandwidth which means that some of the frequency components contained may represent aliased frequencies. However, the considerable integration time of the latest low moment gate reduces this problem significantly.
- Other noise sources than power line noise may contribute to the total noise spectral density in the data at the power transmission frequency. When power line noise is present it tends to dominate all such other noise sources.
- The presented PLNI values are not corrected for fly height or frame angles, which means that adjacent lines crossing the same power line may not exhibit the same values of PLNI.

An example of the grid of the PLNI channel is seen on
Figure 6. Geosoft PLNI map and grid is included in the digital data delivery catalouge.

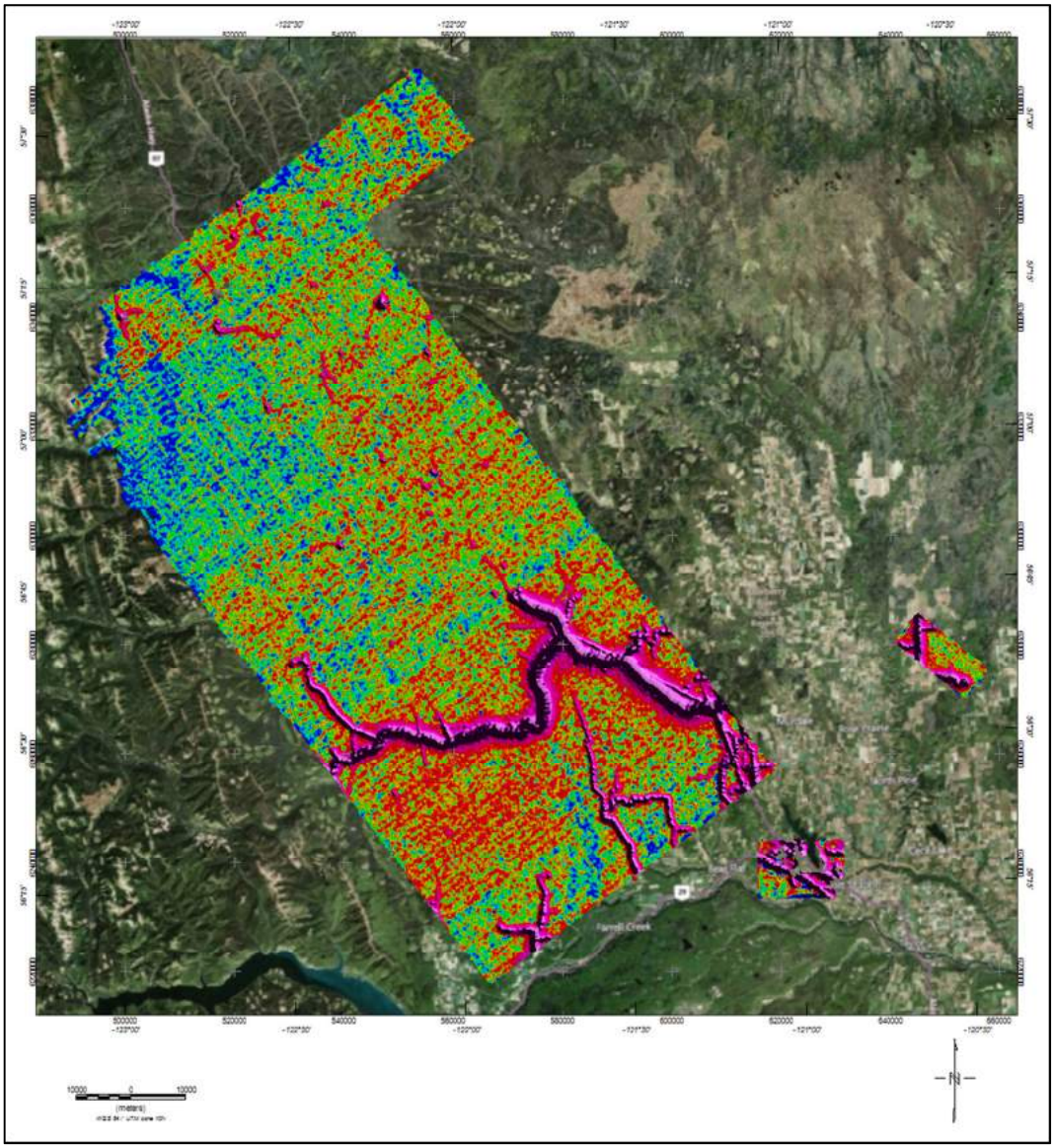

Figure 6 PLNI of Peace Project. Warm colours (red) represent high intensity. UTM Zone 10N *(WGS84).*

Geosoft GDB

The EM GDB file is the final result of the SkyTEM survey, containing all the collected and processed EM data and information used for the interpretation and inversion.

Data in the file is split at the beginning and end of each planned flight line.
The raw EM data and auxiliary data are filtered and processed as described above. All parameters in the GDB-file hence refer to the origin of the frame.

The GDB can be used as input for further processing and gridding and as input to inversion and interpretation software.

The projection of the GDB is given as Latitude/Longitude, WGS84 and UTM Zone 10N (WGS84).

The header of the EM GDB-file gives the following information:

Parameter	Explanation	Unit
Fid	Unique Fiducial number	seconds
Line	Line number	LLLLLL
Flight	Name of flight	yyyymmdd.ff
DateTime	DateTime format	Decimal days
Date	Date	yyyymmdd
Time	Time	hhmmss.zzz
AngleX	Angle in flight direction	Degrees
AngleY	Angle perpendicular to flight direction	Degrees
Height	Filtered height measurement	Meters
Lon	Latitude/Longitude, WGS84	Decimal degrees
Lat	Latitude/Longitude, WGS84	Decimal degrees
E	UTM Zone 10N (WGS84)	Meter
N	UTM Zone 10N (WGS84)	Meter
DEM	Digital Elevation Model	M. a. sl.
Alt	DGPS Altitude	M. a. sl.
GdSpeed	Ground Speed	[km/h]
Curr_LM	Current, low moment	Amps
Curr_HM	Current, high moment	Amps
LM_Z_G01[xx]*	Normalized LM Z-coil value	pV/(m4*A)
HM_Z_G01[xx]*	Normalized HM Z-coil value	pV/(m4*A)
LM_X_G01[xx]*	Normalized LM X-coil value	pV/(m4*A)
HM_X_G01[xx]*	Normalized HM X-coil value	pV/(m4*A)
PLNI	Amplitude spectral density of the power line noise 60 Hz	-
Bmag_Raw	Total Magnetic Intensity – raw magnetic data – magnetic base station	-
Diurnal	Diurnal variation - magnetic base station data	nT
Mag_Raw	Raw magnetic data – total magnetic intensity	nT
Mag_Cor	Residual magnetic field – filtered and corrected for diurnal.	nT
RMF	Total magnetic intensity – final corrected data. IGRF recalculated.	nT
TMI	Total Magnetic Intensity	nT

*) Geosoft array channels are exported, the numbers in the brackets starts from [0]. The first values of each array for each EM channel are blanks as the first gates are still affected by the turn-off of the current. The number in the channel name refer to the first usable gate number.

Presentation of GDB-files

High and low moment z coil gates from the GDB-file have been exported as Geosoft .grd files. The files are included in the data delivery catalogue. Figure 7 shows an example of the HM data. The EM data in the grids have been height corrected in order to minimize the effect of varying magnitude of the EM signal as a function of varying flight height. All data for the gridding was corrected to a flight height of 50m.

Please note that no height correction has been applied to the raw EM data present in the data base.

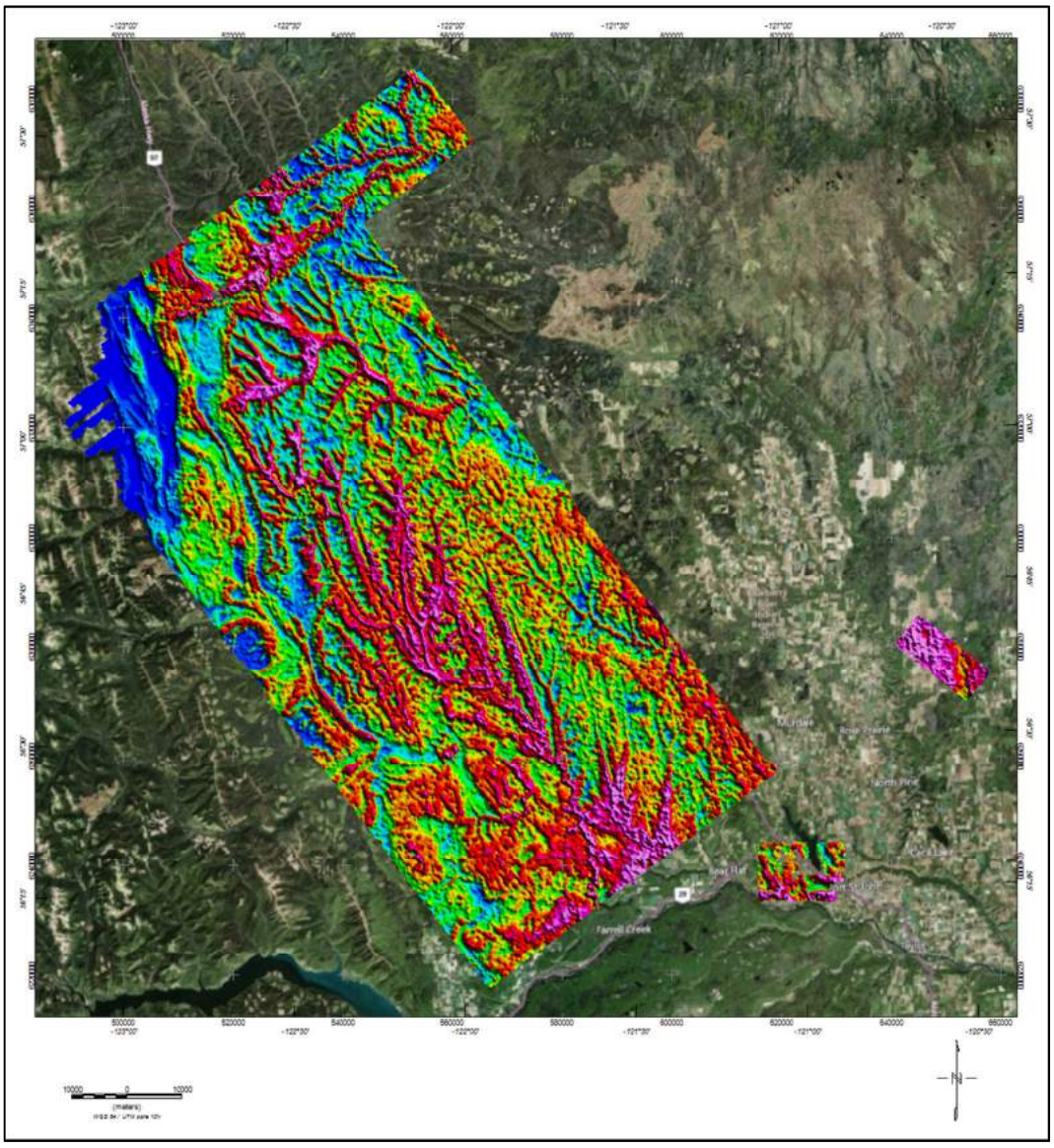

Figure 7. High Moment Z coil (gate 19). Warm colours represent high signal.

Magnetic data

Mag processing

Final processing of the magnetic data involved the application of traditional corrections to compensate for diurnal variation and heading effects prior to gridding. Advanced full processing of magnetic data was implemented in Geosoft's Oasis Montaj software as follows:

- Processing of static magnetic data acquired on magnetic base station
- Pre-processing of airborne magnetic data
    - Stacking of data to 10 Hz in SkyLab.
    - Moving positions to the center of the sensor in SkyLab.
- Processing and filtering of airborne magnetic data
- Standard corrections to compensate the diurnal variation and heading effect
- IGRF correction
- Advanced levelling (careful levelling and micro levelling)
- Gridding

Processing of base station magnetic data

The base station magnetometer data was transferred into the base station Geosoft GDB database on a daily basis for further processing.

The following filter parameters were used:

- Manual despiking to remove spikes
- Fraser Low-pass filter (width 30 sec)
- IRGF correction
    - IRGF: coefficients defined by IGRF 11th generation
    - Date: variable according to date of acquired data
    - Position: fixed GPS WGS84 longitude, latitude and elevation of magnetic base station

Processed residual magnetic data from magnetic base station representing short term variations was merged together with airborne magnetic data using the date and UTC time as reference channels.

Processing and Filtering of airborne magnetic data

Mag data was filtered using a non-linear filter in order to minimize the influence of cultural noise and interpolated as follows:

- Manual despiking to remove spikes and spurious data
- Non-linear filter – width = 100, Filter Tolerance = 0.5
- B-spline – Tension=0.7, Smoothness=0.7

Corrections to the magnetic data

The processing of the airborne magnetic data involved the application of the following corrections:

- Correction for diurnal variation using the digitally recorded ground base station magnetic values as described above
- Lag was negligible and no correction was performed on data.
- Heading effect was negligible and no heading correction was made.

IGRF correction

Geosoft Oasis Montaj Levelling Toolkit was used for applying corrections and levelling on magnetic data.

The International Geomagnetic Reference Field (IGRF) is a long-wavelength regional magnetic field calculated from permanent observatory data collected around the world. The IGRF is updated and determined by an international committee of geophysicists every 5 years. Secular variations in the Earth's magnetic field are incorporated into the determination of the IGRF.

The IGRF model was calculated before levelling using the following parameters for the survey area:

IGRF model year: IGRF 11th generation
Date: variable according to date channel in database
Position: variable according to GPS WGS84 longitude and latitude
Elevation: variable according to magnetic sensor altitude derived from DGPS data

Tie-line levelling and micro-levelling of magnetic data

After applying the above corrections to the profile data, statistical levelling of control lines followed by full levelling of traverse lines and micro-levelling was applied as a standard procedure.

As a part of this levelling procedure, intersections between control and traverse lines were determined.

TMI recalculation

The outcome of processed magnetic data after all corrections and levelling is the Residual magnetic field (RMF).

Total magnetic intensity (TMI) was recalculated to mean sea ellipsoidal level altitude by adding the IGRF regional field back to RMF.

Gridding of magnetic data

The corrected data was used to generate the Residual Magnetic Field (RMF) and Total Magnetic Intensity (TMI) grid. Corrected magnetic line data was interpolated between survey lines using a minimum curvature gridding algorithm to yield x-y grid values.

Figure 8 show gridded data after processing from the magnetometer. All grids and maps from the area (RMF and TMI) can be found in the data delivery folder.

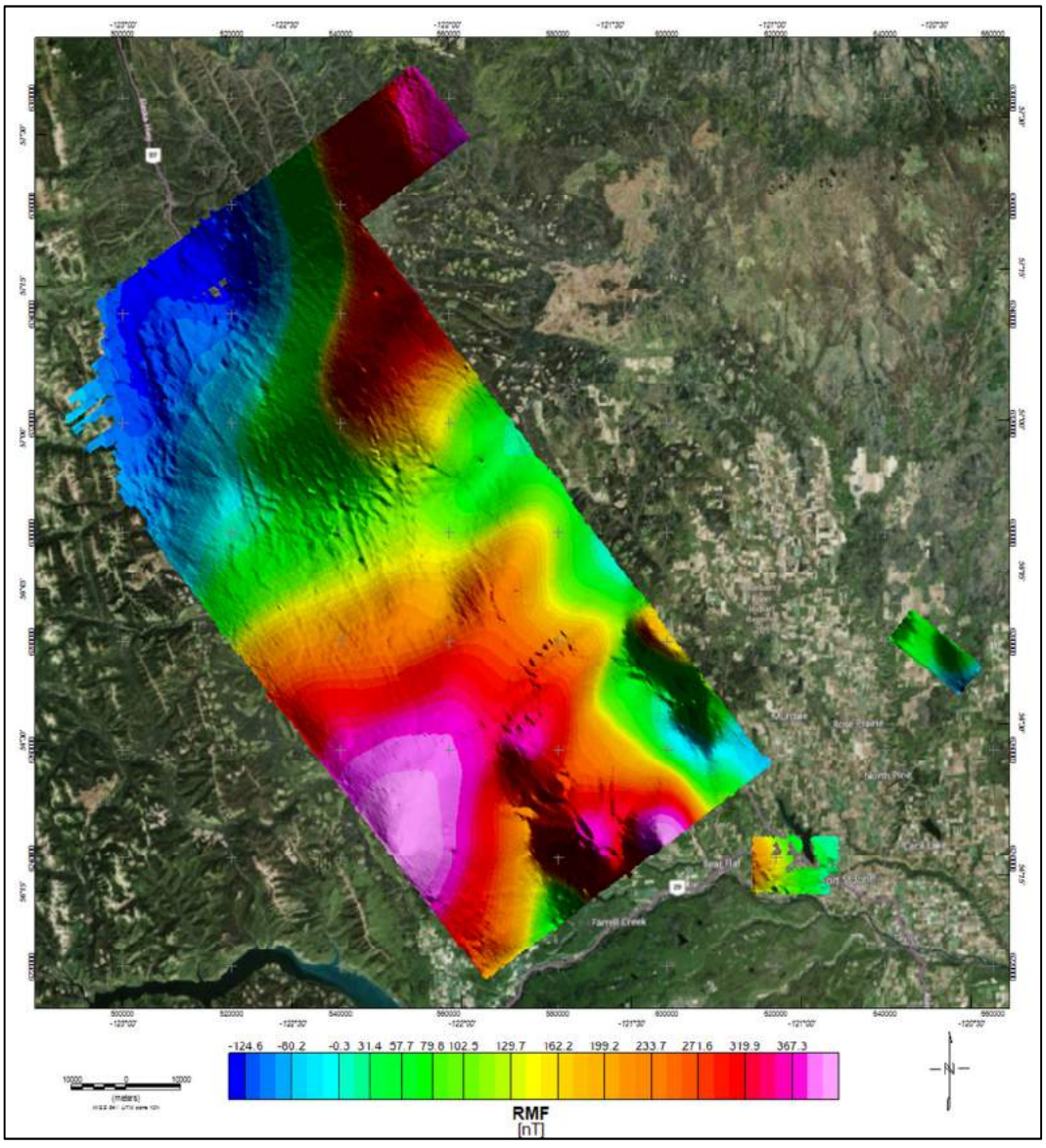

Figure 8 RMF grid of the survey area.

Inversion of the TEM data

In this section, the particulars of modelling and inversion of SkyTEM data from British Columbia, Canada will be described with reference to the more general material found in Appendix 4.

Inversion

The SkyTEM data have been processed and inverted using a laterally constrained inversion (LCI) in Aarhus Workbench, a unique software package initially developed at Aarhus University, Denmark. In this LCI algorithm (Auken et al. 2005), a group of time-domain EM (TEM) soundings are inverted simultaneously using 1-D models. Each sounding yields a separate layered model, but the models are constrained laterally.

The result of the LCI inversion is a quasi-2D model section that varies smoothly along the profile and yields a conductivity model that combines the very good shallow depth resolution offered by the low moment data and the larger depth of investigation from the high moment data.

Initial model and optimisation norm

The LCI code is run in multi-layer, smooth-model mode in which the layer thicknesses are fixed and the data are inverted only for resistivity.
In the inversion the thickness of the first layer is set to 2 m and the depth to the top of the deepest layer boundary is 500 m. While computing the layer thicknesses, the first and last layer boundary scales the model thicknesses automatically using a log distribution. Thicknesses and depths to the top of each layer for the current project are given in the table below.
The input data to the inversion are the LM & HM moments of the Z-component of EM data. The initial model resistivity structure is a homogenous half-space model with an Auto Calculated starting resistivity.

Manually masking of data displaying coupling effects e.g. due to power lines is not part of the current project and therefore cultural effects in the EM data can be present in the final data base.

Layers used in the inversion:

Layer #	Layer Thickness [m]	Depth to top of layer [m]
1	2.0	0.0
2	2.3	2.0
3	2.5	4.3
4	2.9	6.8
5	3.2	9.7
6	3.7	12.9
7	4.1	16.6
8	4.7	20.7
9	5.2	25.3
10	5.9	30.6
11	6.7	36.5
12	7.5	43.2
13	8.5	50.7
14	9.6	59.2
15	10.8	68.8
16	12.2	79.9
17	13.8	91.9
18	15.5	105.7
19	17.5	121.2
20	19.8	138.7
21	22.3	158.5
22	25.2	180.8
23	28.4	206.0
24	32.1	234.4
25	36.2	266.5
26	40.8	302.7
27	46.0	343.5
28	51.9	389.5
29	58.6	441.4
30	-	500.0

Inversion results

The results of the inversions are presented in a GDB file included in the data delivery catalogue. The files contain the resistivities for each layer in the model. The header of the GDB file is described in the table below.

Parameter	Explanation	Unit
Line	Line number	LLLLLL
E	UTM Zone 10N (WGS84)	Meter
N	UTM Zone 10N (WGS84)	Meter
DEM	Digital Terrain Model (Unlevelled)	Meters above mean sea level
ResI1	Residual of data	-
Height	Filtered Height Measurement	Meter
InvHei	Inverted Height	Meter
DOI	Depth of Investigation	-
Elev[xx] *)	Elevation of top of layer xx	Meter
Con[xx] *)	Conductivity of layer xx	S/m
Con[xx]_doi*)	Masked below DOI of layer xx	S/m
RUnc[xx] *)	Relative uncertainty of layer xx	-

*) If Geosoft array channels are exported, the numbers in the brackets starts from [0]

Presentations - Model sections and maps

The models resulting from the inversion are presented as model sections/profiles and as grids of mean conductivity in depth intervals and are delivered in digital format.

Model sections

The model sections can be found in the data delivery folder as PNG's.

The model section plot consists of four subplots as seen in Figure 9. The top plot shows the inverted models, with topography, where the conductivity of the individual layers is colour coded according to the colour bar. The conductivity is shown on a logarithmic scale and conductive and resistive features appear with the same weight. The white shading in the analysis section indicates the estimated depth of investigation (DOI).
The measured and inverted flight elevation is shown with a black and blue line, respectively, above the model section.

Where the colour fades into the white, the inverted conductivity is determined almost exclusively by the regularization, i.e. the conductivity is essentially undetermined.

Below the model section are two plots of the measured data (dots) together with the response of the inverted models (solid lines). LM is low moment data and HM is high moment data. Below the gate plots is a plot of the data residual (black line) of the inversions.

Blank sections in the profile indicates areas where the signal to noise ratio has been too low for any data to be used in the inversion. Essentially the resistivity in those sections can be considered as "Very high" (>1000 Ωm). Alternatively a man-made conductor has interfered with the signal which can also lead to data being discarded prior the inversion.

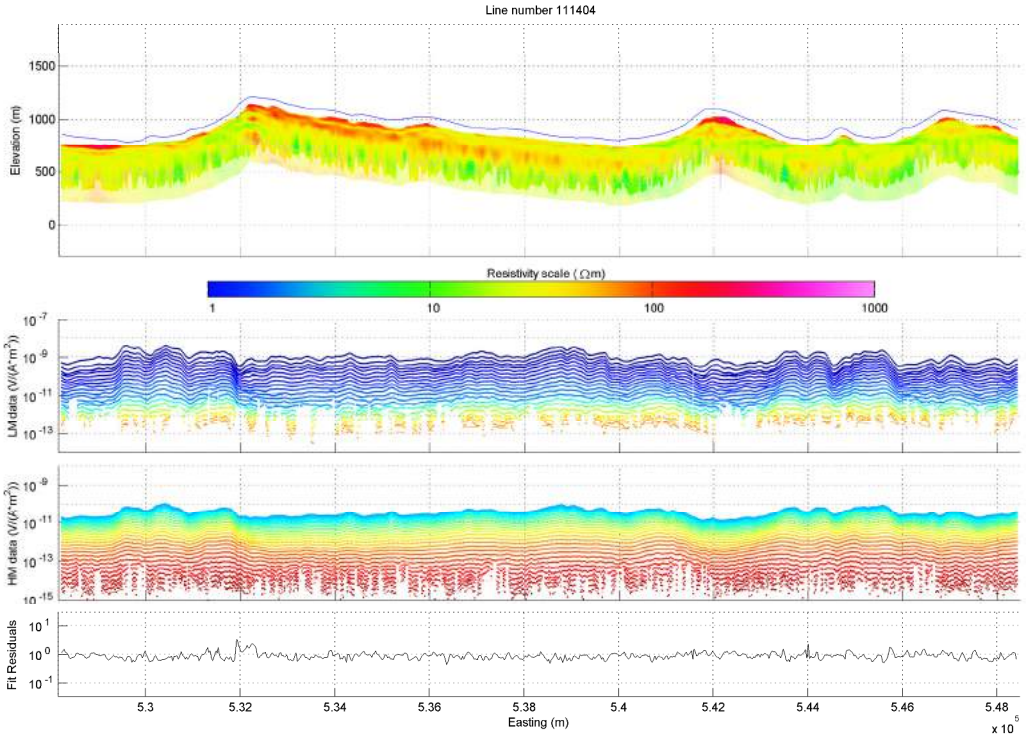

Figure 9 Model section. From top to bottom: Conductivity section with flight height and Depth of Investigation (DOI), LM gate plot (data=dots, model=line), HM gate plot (data=dots, model=line), data residual.

Residuals

The quality of the inversion results can be evaluated by inspecting the residuals. The data residual is calculated by comparing the measured data with the response of the resulting model after inversion. If the residual is in the range of 1, the misfit between the response of the final model and the data is, on average, equal to the noise. If the residual is high, it might be caused by data that are noisier than the noise model takes into account. This can be seen where resistivities are very high and the signal consequently very low. A high data residual can also be due to the inconsistency between the 1D model assumed in the inversion and the 2D/3D character of the real world. These are found primarily at the edges of sharp lateral conductivity contrasts. Finally, coupling effects due to power lines and other manmade conductors can also be a source of a high residual.

Layer Conductivity Maps

The conductivity maps can be found in the data delivery folder as PDF's as well as geosoft.map files.

The conductivity maps show the inverted conductivity for each of the model layers.

As the thickness of the model layers increases downwards the maps represent a varying thickness interval. The depth interval is stated on the files and is in meters below the surface. An example can be seen in
Figure *10*

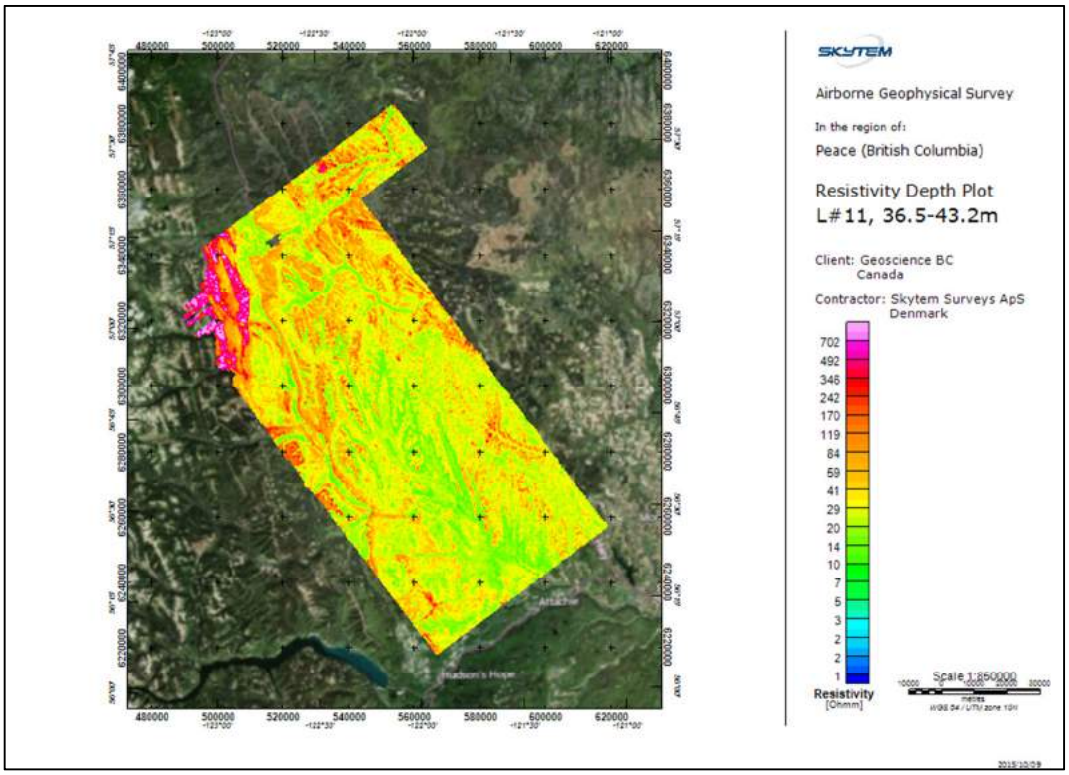

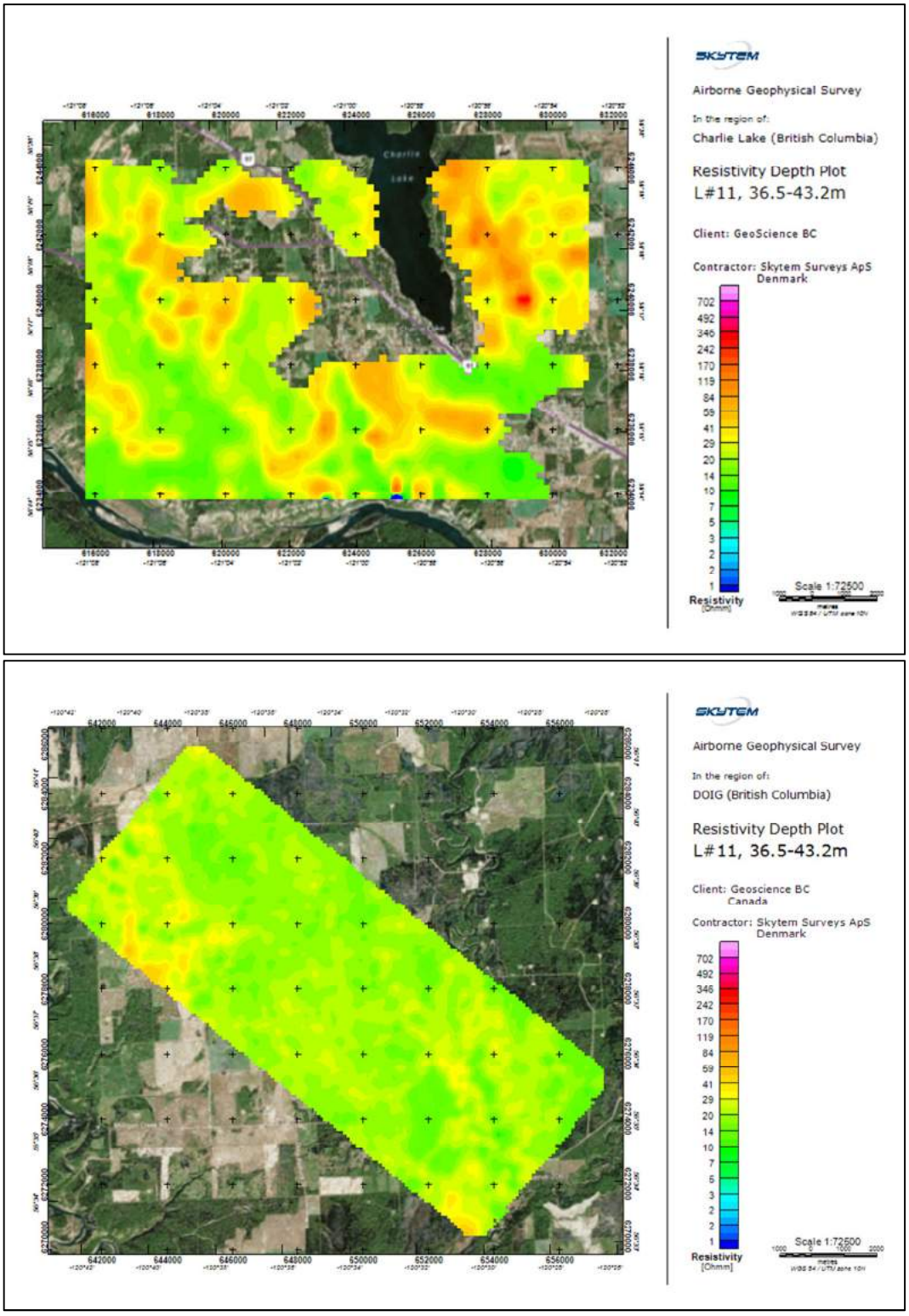

Figure 10 Layer conductivity maps for layer 11

References

Aarhus University, n.d., Guide to 1D-LCI inversion.

Auken, E., Foged, N. and Sørensen, K., 2002, Model recognition by 1-D laterally constrained inversion of resistivity data: Proceedings – New Technologies and Research Trends Session, 8th meeting, EEGS-ES.

Auken, E., Christiansen, A. V., Jacobsen, B. H., Foged, N., and Sørensen, K. I., 2005, Piecewise 1D Laterally Constrained Inversion of resistivity data: *Geophysical Prospecting*, 53, 497–506.

Christiansen, A.V. and Auken, E., 2012, A global measure for depth of investigation: *Geophysics,* vol 77, No. 4, 171-177.

Sattel, D., 2005, Inverting airborne electromagnetic (AEM) data with Zohdy's method, Geophysics, 70, G77-G85.

Sorensen, K. I. and Auken, E.,2004. SkyTEM - A new high-resolution helicopter transient electromagnetic system, Exploration Geophysics, 35, 191-199.

Appendix list

Appendix 1: Instruments

Instrument positions

The instrumentation involves a time domain electromagnetic system, two inclinometers, two altimeters an airborne magnetometer and two DGPS'.

The measurements were carried out, using a setup as described below.

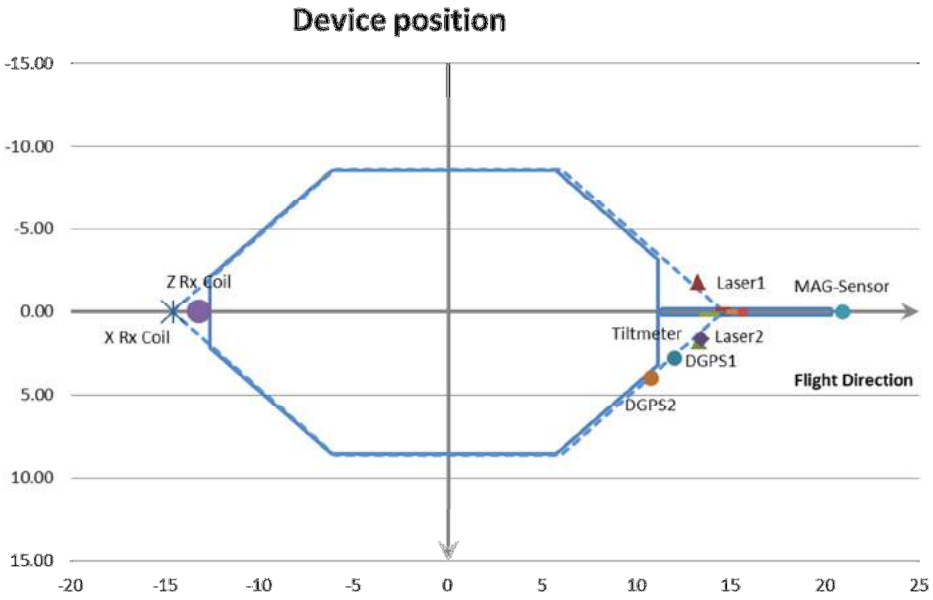

Figure 1 Sketch showing the frame and the position of the basic instruments. The blue line defines the transmitter loop. The horizontal plane is defined by (x, y).

The location of instruments in respect to the frame is shown in Figure 1 and is given in (x, y, z) coordinates in the table below.

X and y define the horizontal plane. Z is perpendicular to (x, y). X is positive in the flight direction, y is positive to the right of the flight direction, and z is positive downwards.

The generator used for powering of the transmitter is ~20 m below the helicopter.

Device	X	Y	Z
DGPS1 (EM)	11.86	2.73	-0.13
DGPS2 (EM)	10.70	3.85	-0.13
HE1 (altim.)	12.97	-1.85	-0.14
HE2 (altim.)	12.97	1.80	-0.14
Inclinometer 1	12.81	1.64	-0.12
Inclinometer 2	12.81	1.64	-0.12
RX (Z Coil)	-13.40	0.00	-2.02
RX (X Coil)	-14.79	0.00	0.00
Mag sensor	20.64	0.00	-0.48

For the location of instruments see Figure 1.

Transmitter

The time domain transmitter loop can be described as an octagon with the corners listed below:

X	Y
-12.64	-2.13
-6.15	-8.59
5.74	-8.59
11.13	-3.19
11.13	3.19
5.74	8.59
-6.15	8.59
-12.64	2.13

The total area of the transmitter coil defined by the corner points is 337.04 m² and 67.87 m in circumference.

The key parameters defining the transmitter set up are:

Low moment

Parameter	Value
Number of transmitter turns	2
Transmitter area	337.04 m²
Peak current	5.8 A
Peak moment	~ 3,000 NIA
Repetition frequency	210 Hz (312.5 Hz)*
On-time	800 µs
Off-time	1581 µs
Duty cycle	33 %
Wave form	Square

* Repetition frequencies are stated as 312.5 Hz in the geometry file used for importing data into the "Aarhus Workbench" software. The software requires a repetition frequency = $(4*\text{OnTime})^{-1}$.

High Moment

Parameter	Value
Number of transmitter turns	12
Transmitter area	337.04 m²
Peak current	118.7 A
Peak moment	~ 490,000 NIA
Repetition frequency	30 Hz (62.5 Hz)*
On-time	4000 µs
Off-time	12667 µs
Duty cycle	24 %
Wave form	Square

* Repetition frequencies are stated as 62.5 Hz in the geometry file used for importing data into the "Aarhus Workbench" software. The software requires a repetition frequency = $(4*\text{OnTime})^{-1}$.

Figure 2 The 337.04 m² frame in production mode.

Receiver system

The decay of the secondary magnetic field is measured using two independent active induction coils. The Z coil is the vertical component, and the X coil is the horizontal in-line component. Each coil has an effective receiver area of 105 m² (Z), 115 m² (x).

The receiver coils are placed in a null-position:

Z coil (x, y, z) = (-13.4 m, 0.0 m, -2.0 m)
X coil (x, y, z) = (-14.76, 0.0 m, 0.0 m)

In the null-position, the primary field is damped with a factor of 0.01 on HM and due to PFC correction it can be neglected on LM.

Figure 3 Rudder containing the Z coil located in the top part of the tower.

The key parameters defining the receiver set up are:

Receiver parameters		
Sample rate		All decays are measured
Number of output gates		37 (HM) and 28 (LM)
Receiver coil low pass filter		210 kHz (Z-coil) and 250 kHz (X-coil)
Receiver instrument low pass filter		300 kHz
Repetition frequency	LM HM	210 Hz 30 Hz
Front gate	LM HM	0.0 µs 370 µs

Receiver gate times are measured from the start of the transmitter current turn-off. A complete list describing gate open, close and centre times are listed in Appendix 2.

Inclination

Instrument type: Bjerre Technology

The inclination of the frame is measured with 2 independent inclinometers. The x and y angles are measured 2 times per second in both directions. The inclinometers are placed in the rear of the frame as close to the z coil as possible, see Figure 1.

The angle data are stored as x, y readings. X is parallel to the flight direction and positive when the front of the frame is above horizontal. Y is perpendicular to the flight direction and negative when the right side of the frame is above horizontal.

The angle is checked and calibrated manually within 1.0 degree by use of a level meter.

DGPS airborne unit and base stations

Chipset: OEMV1-L1 14-channel rate.
Antenna: Trimble, Bullet III GPS Antenna

The differential GPS receiver is on top of the boom in front of the frame.

The DGPS delivers one dataset per second. The raw coordinates are given in Latitude/Longitude, WGS84.

The uncertainty in the xyz-directions is ± 1 m after processing.
The processed DGPS data is combined with the EM data in the xyz-files, giving the precise position.

DGPS parameters	
Sample rate	1 Hz
Uncertainty	± 1 m

Altimeter

Instrument type: MDL ILM300R

Two independent laser units mounted on the frame measuring the distance from the frame to the ground, see Figure 1

Each laser delivers 30 measurements per second, and covers the interval from 0.2 m to approximately 200 m.

Dark surfaces including water surfaces will reduce the reflected signal. Consequently, it may occur that some measurements do not result in useful values.

The altimeter measurements are given in meters with two decimals. The uncertainty is 10 - 30 cm. The lasers are checked on a regular basis against well-defined targets.

Laser parameters	
Sample rate	30 Hz
Uncertainty	10 - 30 cm
Min/ max range	0.2 m / 200 m

Magnetometer airborne unit

Instrument type: Geometrics G822A sensor and Kroum KMAG4 counter.

The Geometrics G822A sensor and Kroum KMAG4 counter is a high sensitivity cesium magnetometer. The basic of the sensor is a self-oscillating split-beam Cesium Vapor (non-radioactive) Principe, which operates on principles similar to other alkali vapor magnetometers.

The sensitivity of the Geometrics G822A sensor and Kroum KMAG4 counter is stated as <0.0005 nT/√Hz rms. Typically 0.002 nT P-P at a 0.1 second sample rate, combined with absolute accuracy of 3 nT over its full operating range.

The magnetometer is synchronized with the TEM system. When the TEM signal is on, the counter is closed. In the TEM off-time the magnetometer data is measured from 2500 microseconds until the next TEM pulse is transmitted. The data are averaged and sampled as 60 Hz.

Parameter	Value
Sample frequency	60 Hz (in between each HM EM pulse)
Magnetometer on	HM Cycles
Magnetometer off	LM Cycles

Magnetometer base station

Instrument type: GEM Overhauser (GEM Proton used as backup).

The GEM Overhauser (GEM Proton used as backup) is a portable high-sensitivity precession magnetometer.

The GEM Overhauser (GEM Proton used as backup) is a secondary standard for measurement of the Earth's magnetic field with 0.01 nT resolutions, and 1 nT absolute accuracy over its full temperature range.

The base station data are sampled with 1 Hz frequency.

Appendix 2: Time gates

Gate	GateOpen (µs)	GateClose (µs)	Gatewidth (µs)	Raw GateCenter	GateCenter (Applied time shift calibra-tion) (µs)	Comment
1	0.430	1.000	0.570	0.715	-1.465	Not Used
2	1.430	3.000	1.570	2.215	0.035	Not Used
3	3.430	5.000	1.570	4.215	2.035	Not Used
4	5.430	7.000	1.570	6.215	4.035	Not Used
5	7.430	9.000	1.570	8.215	6.035	Not Used
6	9.430	11.000	1.570	10.215	8.035	Not Used
7	11.430	13.000	1.570	12.215	10.035	Not Used
8	13.430	16.000	2.570	14.715	12.535	Not Used
9	16.430	20.000	3.570	18.215	16.035	Not Used
10	20.430	25.000	4.570	22.715	20.535	LM Only
11	25.430	31.000	5.570	28.215	26.035	LM Only
12	31.430	39.000	7.570	35.215	33.035	LM & HM
13	39.430	49.000	9.570	44.215	42.035	LM & HM
14	49.430	62.000	12.570	55.715	53.535	LM & HM
15	62.430	78.000	15.570	70.215	68.035	LM & HM
16	78.430	98.000	19.570	88.215	86.035	LM & HM
17	98.430	123.000	24.570	110.715	108.535	LM & HM
18	123.430	154.000	30.570	138.715	136.535	LM & HM
19	154.430	194.000	39.570	174.215	172.035	LM & HM
20	194.430	245.000	50.570	219.715	217.535	LM & HM
21	245.430	308.000	62.570	276.715	274.535	LM & HM
22	308.430	389.000	80.570	348.715	346.535	LM & HM
23	389.430	490.000	100.570	439.715	437.535	LM & HM
24	490.430	617.000	126.570	553.715	551.535	LM & HM
25	617.430	778.000	160.570	697.715	695.535	LM & HM
26	778.430	980.000	201.570	879.215	877.035	LM & HM
27	980.430	1235.000	254.570	1107.715	1105.535	LM & HM
28	1235.430	1557.000	321.570	1396.215	1394.035	LM & HM
29	1557.430	1963.000	405.570	1760.215	1758.035	HM Only
30	1963.430	2474.000	510.570	2218.715	2216.535	HM Only
31	2474.430	3119.000	644.570	2796.715	2794.535	HM Only
32	3119.430	3932.000	812.570	3525.715	3523.535	HM Only
33	3932.430	4957.000	1024.570	4444.715	4442.535	HM Only
34	4957.430	6249.000	1291.570	5603.215	5601.035	HM Only
35	6249.430	7877.000	1627.570	7063.215	7061.035	HM Only
36	7877.430	9931.000	2053.570	8904.215	8902.035	HM Only
37	9931.430	12202.000	2270.570	11066.715	11064.535	HM Only

Note: The first gates are not used in any of the moments in the present survey as it is in the transition zone.

HM gate times are shifted 350 µs (end of turnoff ramp) in respect to the gate times. Workbench applies this time shift automatically while defined in the geometry file.

Appendix 3: Calibration of the TEM system

Waveform

The waveform is measured with a 60 Hz script with a repetition frequency of 210 Hz for LM and with a repetition frequency of 30 Hz for HM. Figure 1 and Figure 2 show the up and down ramp.

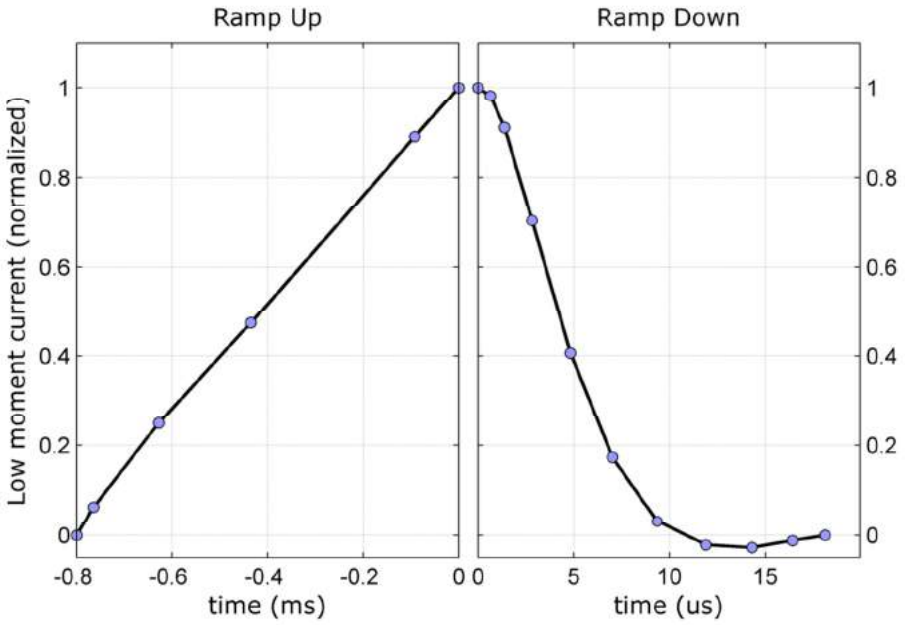

Figure 1 Ramp up and down at 210 Hz (LM). The current is normalised.

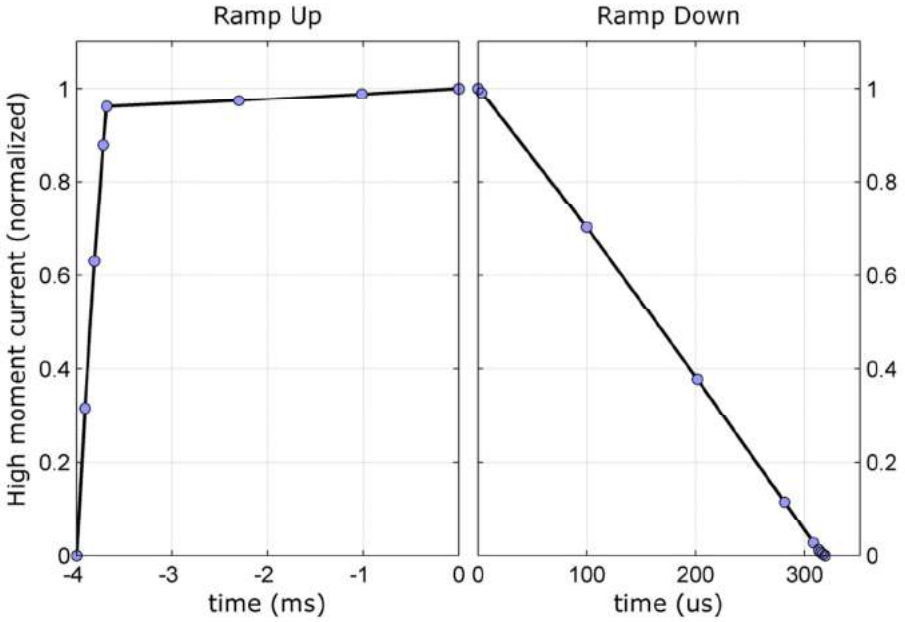

Figure 2 Ramp up and down at 30 Hz (HM). The current is normalised.

The waveform is measured using a current probe (turn-on ramp) and a pick-up coil (outputs dI/dt) for the (turn-off ramp). The approximation to the measured waveform can be applied in modelling of the data, which was also the case for inversion of the survey data in this report, see table 1 and 2 for details.

LM

Parameter	Value
Base frequency	210 Hz
Current range	6 A

Table 1: Waveform parameters for LM

Time [s]	Normalized current
-8.0000e-004	0.00000E+000
-7.6473e-004	6.3431e-002
-6.2818e-004	2.4971e-001
-4.3497e-004	4.7453e-001
-9.2197e-005	8.9044e-001
6.6270e-008	1.0000e+000
6.4173e-007	9.8170e-001
1.3872e-006	9.1036e-001
2.8210e-006	7.0394e-001
4.8283e-006	4.0644e-001
7.0076e-006	1.7421e-001
9.3590e-006	3.1535e-002
1.1882e-005	-2.1588e-002
1.4291e-005	-2.7660e-002
1.6413e-005	-1.2070e-002
1.8107e-005	0.00000E+000

Table 2: Normalized current for LM

HM

Parameter	Value
Base frequency	30 Hz
Current range	120 A

Table 3: Waveform parameters for HM

Time [s]	Normalized current
-4.00000E-003	0.00000E+000
-3.91300E-003	3.17153E-001
-3.81313E-003	6.30292E-001
-3.72277E-003	8.79197E-001
-3.68473E-003	9.61095E-001
-2.30082E-003	9.73942E-001
-1.01204E-003	9.88394E-001
0.00000E+000	1.00000E+000
3.25433E-006	9.91368E-001
9.99755E-005	7.01860E-001
2.01631E-004	3.77911E-001
2.81574E-004	1.15687E-001
3.08222E-004	2.79070E-002
3.13115E-004	1.21241E-002
3.14989E-004	6.60584E-003
3.16781E-004	3.02920E-003
3.18848E-004	0.00000E+000

Table 4: Normalized current for HM

Calibration

The complete SkyTEM equipment has been calibrated at the National Danish Reference Site. The following plots, Figure 3 to Figure 7, show the measured data as well as the expected response in altitudes: 13 m, 15 m, 23 m, 26 m, 33 m and 36 m.

The reference data for both LM and HM data are shown as grey curves and the measured data for LM and HM as green and blue curves respectively.

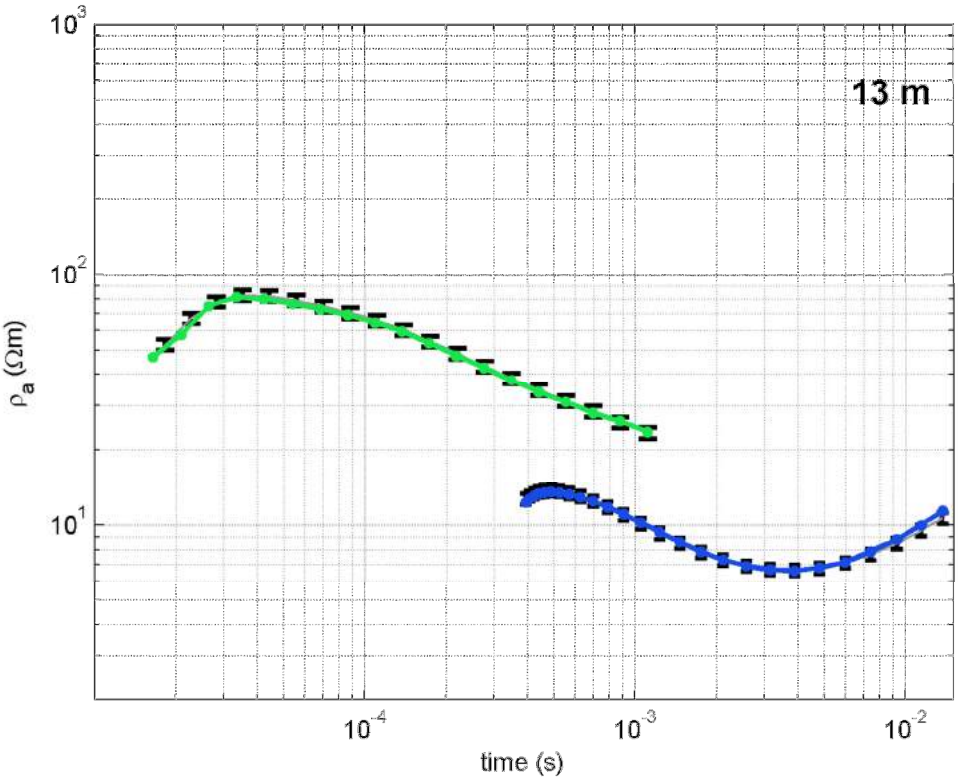

Figure 3 The frame is in 13 m altitude. Grey curves with 5% error bars are the expected response, and green curves (LM) and blue curves (HM) are the actual measurements.

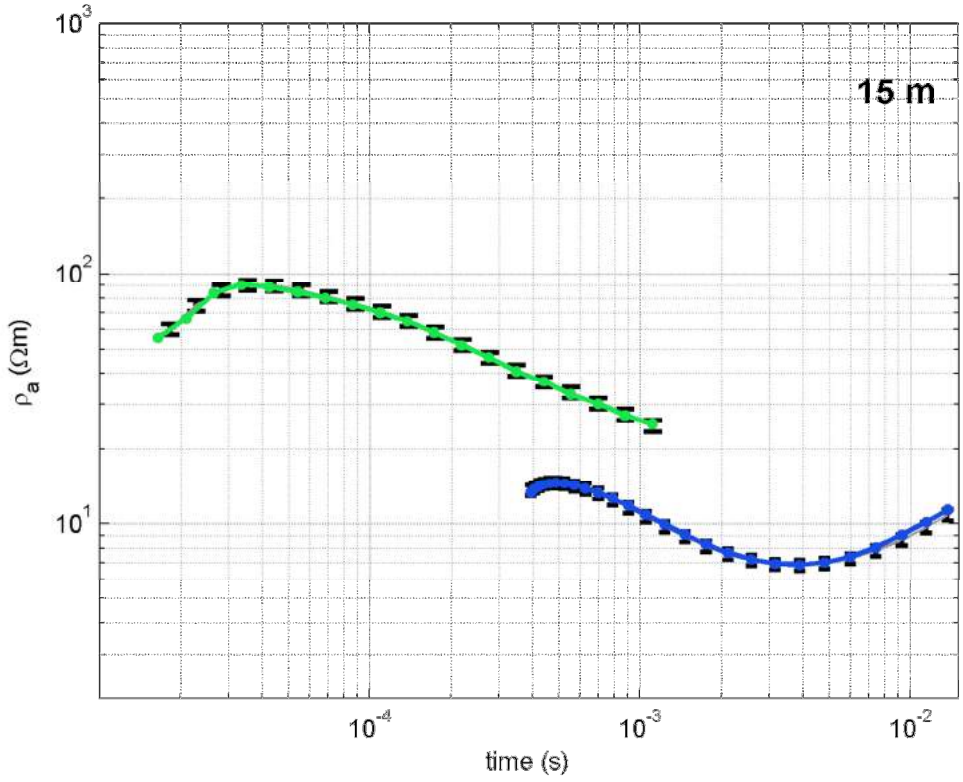

Figure 4 The frame is in 15 m altitude. Grey curves with 5% error bars are the expected response, and green curves (LM) and blue curves (HM) are the actual measurements.

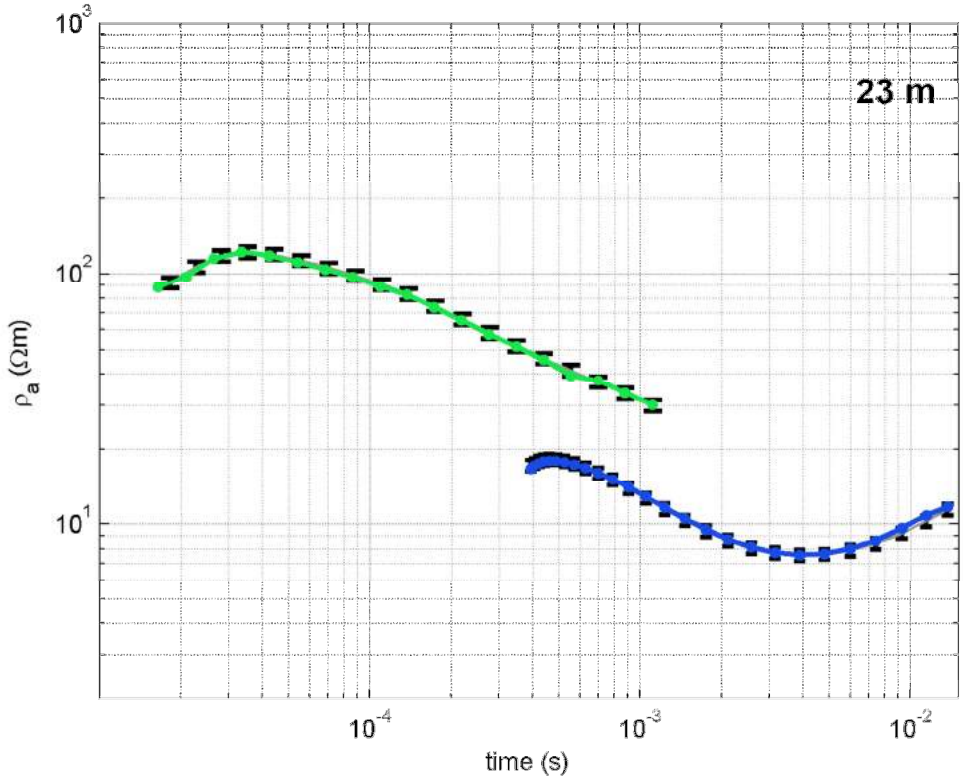

Figure 5 The frame is in 23 m altitude. Grey curves with 5% error bars are the expected response and green curves (LM) and blue curves (HM) are the actual measurements.

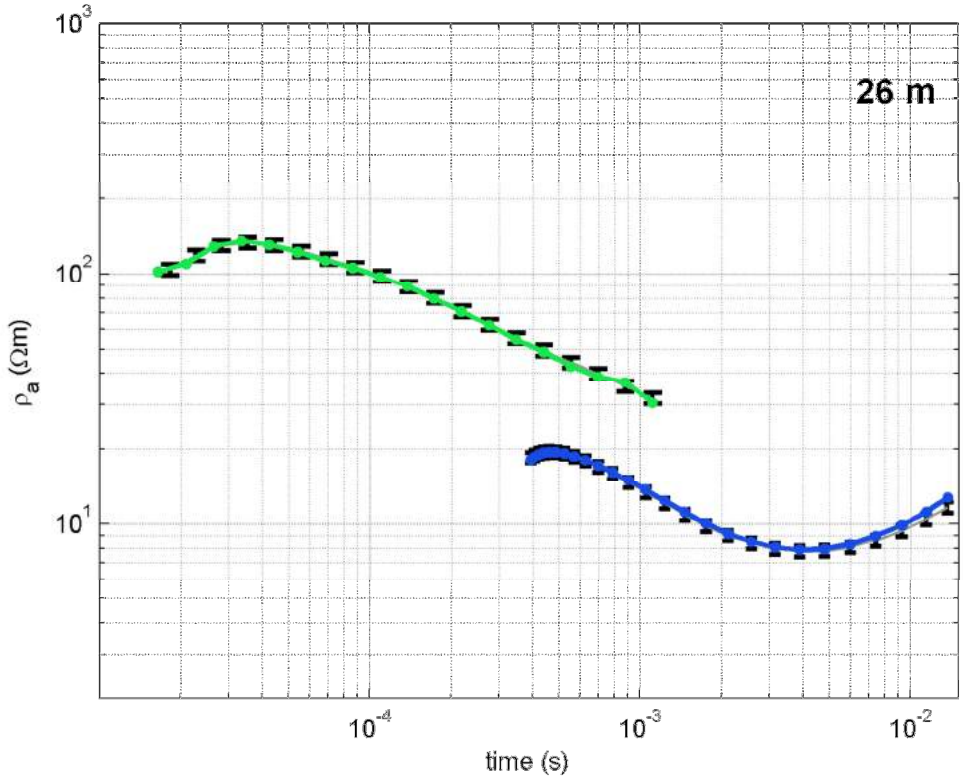

Figure 6 The frame is in 26 m altitude. Grey curves with 5% error bars are the expected response and green curves (LM) and blue curves (HM) are the actual measurements.

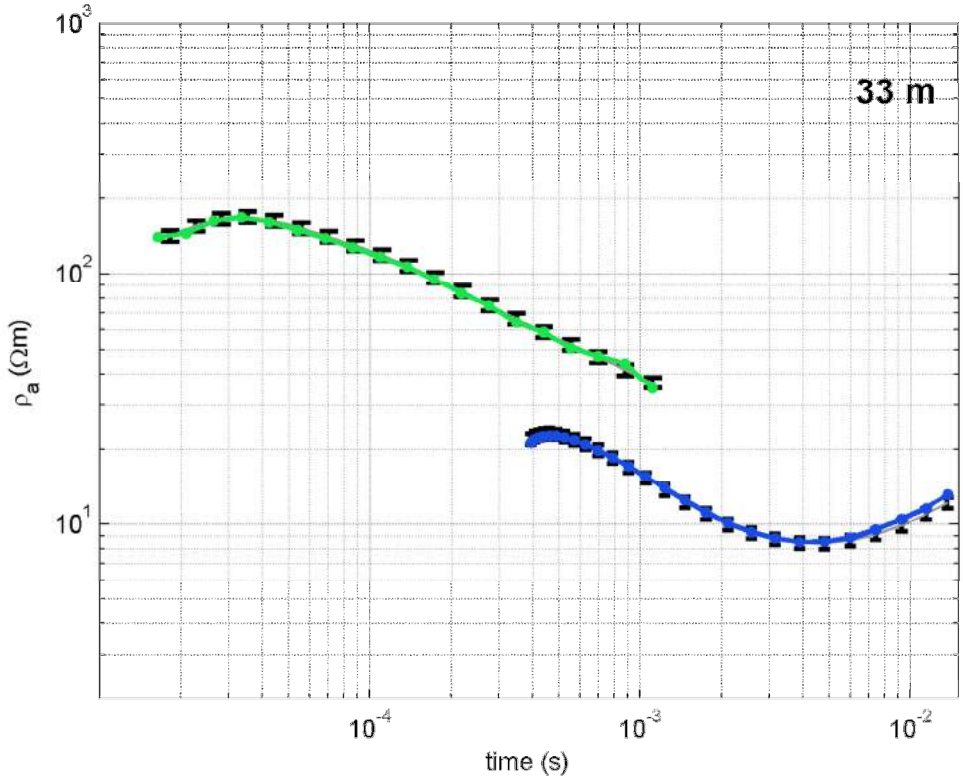

Figure 7 The frame is in 33m altitude. Grey curves with 5% error bars are the expected response and green curves (LM) and blue curves (HM) are the actual measurements.

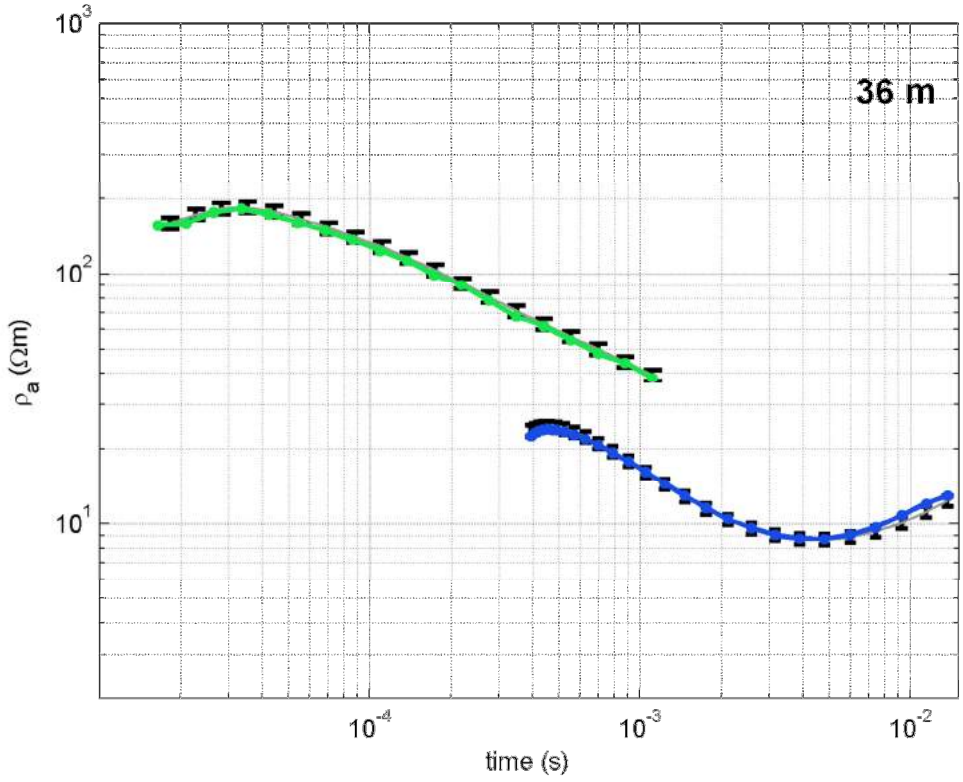

Figure 8 The frame is in 36 m altitude. Grey curves with 5% error bars are the expected response and green curves (LM) and blue curves (HM) are the actual measurements.

Appendix 4: Modelling and Inversion of TEM Data

This appendix gives a brief introduction to modelling and inversion of SkyTEM data.

Model and inversion routine

The SkyTEM data have been processed and inverted using a laterally constrained inversion (LCI) in Aarhus Workbench, a unique software package initially developed at Aarhus University, Denmark. In this LCI algorithm, a group of time-domain EM (TEM) soundings are inverted simultaneously using 1-D models (Auken et al. 2002 & 2005). Each sounding yields a separate layered model, but the models are constrained laterally on resistivity.

The result of the LCI inversion is a quasi-2D model section that varies smoothly along the profile. The LCI inversion is capable of simultaneously inverting the interleaved HM and LM measurements, yielding a conductivity model that combines the very good shallow depth resolution offered by the low moment data and the larger depth of investigation from the high moment data.

The LCI code is run in multi-layer, smooth-model mode, in which the layer thicknesses are fixed and the data are inverted only for resistivity. The LCI smooth-model inversion typically uses 20-30 layers. Smoothness constraints are applied on the variation of resistivity with depth, in additional to the lateral constraints between adjacent models. Multi-layer smooth-model inversion is slower to compute, but is usually able to provide a very close fit to the observed data.
In the model set-up the thickness of the first layer and the depth to the top of the deepest layer boundary is given. While computing the layer thicknesses, the first and last layer boundary scales the model thicknesses automatically using a log distribution.
The input data to the inversion are the LM & HM moments of the Z-component of EM data. Both moments are combined in a single inversion to increase the depth resolution. The initial model resistivity structure is a homogenous half-space model with an Auto Calculated starting resistivity.

Constraints are given as factors, i.e. a factor of 1.1 means that the parameter can vary between the starting value divided by/times 1.1 (Aarhus University).
The LCI inversion allows for horizontal and vertical constraints to be set for resistivities.
Horizontal constraints are scaled by distance using a reference distance and power function:

$$C = 1 + \left(C_{opt} - 1\right)\left(\frac{\Delta GPS}{Dist_{ref}}\right)^{n}$$

Where C is the used constraint, C_{opt} is the optimal constraint at a sounding distance of $Dist_{ref}$ and ΔGPS is the actual sounding distance.
The horizontal constraints are initially scaled by distance and a power function. Inversion for flight altitude is included after the first 5 inversion runs. The constraint on the processed flight height is set low and is only allowed a very limited variation.
The methodology for calculating the DOI is based on a recalculated Jacobian matrix from a 1D model (Christiansen and Auken, 2012). Working with global and absolute threshold values requires a relative, data-type, independent relation between the model space and data space, which we obtain by working in the logarithmic model and data spaces. For a given model, the DOI calculations solely include information from the part of the Jacobian relating to the observed data. This means that lateral or vertical model constraints or a priori information, which also contributes information to the model, is not included. The workflow includes the following steps:
1) Starting from a measured data set, we invert the data into a smooth model. The inversion includes the data uncertainty, estimated from the data stack, and the regularization method of the chosen inversion algorithm.
2) We then calculate the Jacobian for the sub-discretized model.
3) The Jacobian is finally used to compute the cumulated sensitivities from which we can deduct the DOI.

Data and noise model

The inaccuracy of TEM data is influenced by the ambient noise. This noise is reduced by selective stacking of delay time series and by applying appropriate filters in the receiver system.

Data insufficiency

For SkyTEM data, the insufficiency lies primarily in the limited delay time range that can be obtained. The earliest obtainable time gate is determined by the turnoff of the Tx current, and the latest useful time gate is determined by the signal to noise ratio. Increasing the Tx moment will give better measurements at late times, and thus improve the depth penetration, but also increase the turnoff time and thus remove early-time gates, thereby making the near-surface resolution poorer. This trade-off is solved by transmitting an alternating sequence of (1) a low moment that can be turned off quickly to give good near-surface resolution, and (2) a high moment that will improve the signal-to-noise ratio at late times, thus improving depth penetration.

Model inconsistency

When using 1D models in the interpretation of SkyTEM data, inconsistency arises where the lateral gradient of conductivity is not small, e.g. typically in mining applications. However, also in environmental investigations, inconsistencies can arise, typically where near-surface good conductors have abrupt boundaries.

Often such inconsistency is indicated by the data residual being high and one should look upon the inversion results with some caution at these locations. 3D effects can also reveal themselves by the so-called 'pant legs', i.e. conductive or resistive structures projecting at an angle of approximately 30 degrees from the horizontal at the edges of high contrast structures.

Appendix 5: Flight Reports

This appendix gives a report with key information regarding the data acquisition for each flight.

Weather

Flight	Temp. (C)	Wind (m/s)	Visibility	Description
20150710.01	20	5	Good	Good
20150710.02	20	5	Good	Good
20150710.03	20	5	Good	Good
20150711.01	15	2	Good	Light rain
20150711.02	20	2	Good	Good
20150711.03	20	2	Good	Good
20150712.01	20	2	Good	Light rain
20150712.02	20	5	Good	Overcast
20150712.03	25	5-8	Good	Broken clouds
20150712.04	25	5-8	Good	Broken clouds
20150713.01	20	2	Good	Broken clouds
20150713.02	25	5	Good	Broken clouds
20150714.01	15	5	Good	Broken clouds
20150714.02	20	8-10	Good	Broken clouds
20150714.03	20	8-10	Good	Broken clouds
20150714.04	20	8-10	Good	Broken clouds
20150715.01	20	5	Good	Broken clouds
20150715.02	25	8-10	Good	Broken clouds
20150715.03	25	8-10	Good	Broken clouds
20150716.01	25	5	Good	Broken dark clouds, rain at west of block
20150717.01	25	5	Good	Sunny with few clouds
20150718.01	25	5	Good	Broken clouds
20150719.01	25	5	Good	Broken clouds
20150719.02	25	5	Good	Broken clouds
20150719.03	20	0-2	Good	Broken clouds
20150720.01	15	0-5	5-10 km	Overcast, low ceilings and thunderstorms
20150721.01	15	0-5	1-3 km	Overcast, low ceilings
20150722.01	15	0-5	5-10 km	Overcast, low ceilings
20150722.02	15	0-5	5-10 km	Overcast, low ceilings
20150723.01	15	0-2	Good	Broken clouds
20150723.02	15	0-2	Good	Broken clouds
20150723.03	20	5	Good	Broken clouds
20150724.01	20	5	Good	Broken clouds
20150724.02	20	5	Good	Broken clouds
20150724.03	20	5	Good	Broken clouds
20150725.01	25	2-5	Good	Few clouds

20150725.02	25	2-5	Good	Few clouds
20150725.03	25	2-5	Good	Few clouds
20150726.01	20	5	Good	Few clouds
20150726.02	20	5	Good	Few clouds
20150726.03	20	5	Good	Broken clouds
20150727.01	20	5	Good	Broken clouds
20150727.02	20	5	Good	Broken clouds
20150727.03	20	5	Good	Broken clouds
20150727.04	20	5	Good	Broken clouds
20150728.01	20	5	Good	Few clouds
20150728.02	20	5	Good	Few clouds
20150728.03	20	5	Good	Few clouds
20150728.04	20	5	Good	Few clouds, Rain during flight
20150729.01	20	3 - 5	Good	30% Overcast
20150729.02	20	3 - 5	Good	30% Overcast
20150729.03	18	1 - 3	Good	20% Overcast
20150730.01	20	1 - 3	Good	Few clouds
20150730.02	20	1 - 3	Good	Few clouds
20150730.03	20	1 - 3	Good	Few clouds
20150730.04	20	1 - 3	Good	Few clouds
20150730.05	20	1 - 3	Good	Few clouds
20150730.06	20	1 - 3	Good	Few clouds
20150731.01	20	1 - 3	Good	Few clouds
20150731.02	20	1 - 3	Good	Few clouds
20150731.03	20	1 - 3	Good	Few clouds
20150731.04	20	1 - 3	Good	Few clouds
20150801.01	20	1 - 3	Good	Few clouds
20150801.02	20	1 - 3	Good	Few clouds
20150801.03	20	1 - 3	Good	90% overcast some light rain spots
20150801.04	21	1 - 3	Good	90% overcast some light rain spots
20150802.01	20	1 - 3	Good	Few clouds
20150802.02	15	1 - 3	Good	Few clouds
20150802.03	15	1 - 3	Good	Few clouds
20150802.04	15	1 - 3	OK	Light rain outside block
20150804.01	17	1 - 3	Good	Low clouds in the morning, Scattered clouds in the PM
20150804.02	17	1 - 3	Good	Scattered clouds
20150804.03	17	1 - 3	Good	Scattered clouds
20150805.01	15	1 - 3	OK	Light rain outside block
20150805.02	15	1 - 3	OK	Light rain outside block
20150806.01	15	1 - 3	Good	Partly cloudy
20150806.02	15	1 - 3	Good	Partly cloudy

20150806.03	15	1 - 3	Good	Partly cloudy, some rain
20150807.01	16	1 - 5	Ok	Some scattered light rain. Thunderstorm at the end of the flight
20150807.02	18	1 - 5	ok	Some light rain.
20150808.01	14	1 - 3	ok	Some scattered light rain and fog.
20150808.02	16	1 - 3	ok	Light scattered rain
20150808.03	16	1 - 3	ok	Light scattered rain
20150809.01	16	1-3	Good	Partly cloudy
20150809.02	16	1-3	Good	Partly cloudy
20150809.03	16	1-3	Good	Partly cloudy
20150810.01	16	1 - 4	Good	Sunny
20150810.02	18	1 - 4	Good	Sunny
20150810.03	26	5 - 10	Good	Sunny
20150810.04	26	3 - 8	Good	Sunny
20150810.05	23	2 - 7	Good	Sunny
20150811.01	16	2-7	Good	Partly cloudy
20150811.02	16	5-10	Good	Partly cloudy
20150811.03	16	5-10	Good	Partly cloudy
20150811.04	16	5-10	Good	Partly cloudy
20150812.01	16	5-10	Good	Partly cloudy
20150812.02	20	5-10	Good	Partly cloudy
20150812.03	20	5-10	Good	Partly cloudy
20150812.04	20	2 - 5	Good	Partly cloudy
20150812.05	20	2 - 5	Good	Partly cloudy
20150813.01	15	1-5	Good	Partly cloudy
20150813.02	20	1-6	Good	Mostly sunny
20150813.03	20	1-8	Good	Mostly sunny
20150813.04	20	5-10	Good	Mostly sunny
20150813.05	21	2-7	Good	Mostly sunny
20150814.01	16	0-4	Good	10% Overcast. Some fog covered survey area
20150814.02	18	0-5	Good	10% Overcast. A little fog covered survey area
20150814.03	20	1-5	Good	30% Overcast
20150814.04	20	1-5	Good	10% Overcast
20150814.05	18	0-2	Good	Sunny
20150815.01	15	0-3	Good	Mostly sunny
20150815.02	15	1-4	Good	Mostly sunny
20150815.03	15	0-3	Good	Mostly sunny
20150816.01	15	0-3	Good	Partially cloudy
20150816.02	15	0-3	Good	Mostly sunny
20150816.03	20	1-4	Good	Mostly sunny

20150817.01	20	1-4	Good	Partially cloudy
20150817.02	25	1-4	Good	Partially cloudy, then cold front coming in
20150817.03	20	0-2	Good	Partially cloudy
20150818.01	15	0-2	Good	Partially cloudy
20150818.02	15	0-2	Good	Partially cloudy
20150818.03	20	0-2	Good	Mostly sunny
20150818.04	20	0-2	Good	Mostly sunny
20150819.01	10	0-2	Good	Mostly sunny
20150819.02	10	0-2	Good	Mostly sunny
20150819.03	15	0-2	Good	Mostly sunny
20150819.04	15	0-2	Good	Partial cloudy, light rain
20150819.05	15	1-3	Good	Partially cloudy
20150820.01	15	3-5	Good	Overcast with few low clouds
20150820.02	15	3-5	Good	Overcast with few low clouds
20150821.01	10	1-5	Good	Overcast
20150821.02	10	1-5	Good	Overcast
20150821.03	15	1-5	Good	Mostly sunny
20150821.04	15	1-5	Good	Mostly sunny
20150822.01	15	0-4	Good	Sunny
20150822.02	15	0-4	Good	Sunny

Flight Diary

Flight	Comments
20150710.01	Calibration
20150710.02	Calibration
20150710.03	High Altitude
20150711.01	Ferry
20150711.02	Calibration
20150711.03	Production, 1 line, aborted due to generator issues
20150712.01	Production, aborted due to generator issues
20150712.02	Production, 2 lines
20150712.03	Production, aborted due to generator issues
20150712.04	Production, aborted due to generator issues
20150713.01	Production, aborted due to generator issues
20150713.02	Production, aborted due to generator issues
20150714.01	Production, 2 lines
20150714.02	Production, 3 lines
20150714.03	Production, 3 lines
20150714.04	Production, 3 lines
20150715.01	Production
20150715.02	Production
20150715.03	Production
20150716.01	Production, 3 lines, problems after rain encounter

20150717.01	Production, 3 lines
20150718.01	Production on one tie line, one prod line, ferry to Sikanni Chief Airstrip
20150718.02	Ferry from Sikanni Chief airstrip to S3
20150719.01	Production around Pink Mountain Lodge
20150719.02	Production at north-west recreational block
20150719.03	Production at north-west recreational block
20150720.01	Attempted production flight, aborted due to weather
20150721.01	Weather check
20150722.01	Production at north-west recreational block
20150722.02	Production at north-west recreational block, aborted due to weather
20150723.01	Production at north-west recreational block
20150723.02	Production at north-west recreational block
20150723.03	Production at north-west recreational block
20150724.01	Production at north-west recreational block
20150724.02	Production at north-west recreational block
20150724.03	Production at north-west recreational block
20150725.01	Production at north-west recreational block
20150725.02	Production at north-west recreational block
20150725.03	Production at north-west recreational block
20150726.01	Production at north-west recreational block
20150726.02	Production at north-west recreational block
20150726.03	Production at north-west recreational block
20150727.01	Production at north-east recreational block
20150727.02	Production at north-east recreational block
20150727.03	Production at north-east recreational block
20150727.04	Production at north-east recreational block
20150728.01	Production at north-east recreational block
20150728.02	Production at north-east recreational block
20150728.03	Production at north-east recreational block
20150728.04	Production at north-east recreational block
20150729.01	Production at north-east recreational block
20150729.02	Production at north-east recreational block
20150729.03	Production at north-east recreational block
20150730.01	Production at north-east recreational block
20150730.02	HA Test
20150730.03	HA Test
20150730.04	Production at north-east recreational block
20150730.05	Production at north-east recreational block
20150730.06	Production at north-east recreational block
20150731.01	Production at north-east recreational block
20150731.02	Production below north-east recreational block
20150731.03	Production below north-east recreational block
20150731.04	Production below north-east recreational block
20150801.01	Production below north-east recreational block
20150801.02	Production below north-east recreational block
20150801.03	Production below north-east recreational block
20150801.04	Production below north-east recreational block
20150802.01	Production in northeast recreational block (Ties)
20150802.02	Production in northeast recreational block (Ties)

20150802.03	Production in northeast recreational block (Ties)
20150802.04	Production in northeast recreational block (Ties), short due to rain
20150804.01	Production in northeast recreational block (Ties)
20150804.02	Production in northwest recreational block (Ties)
20150804.03	Production in northwest recreational block (Ties)
20150805.01	Production in northwest recreational block (Ties)
20150805.02	Production in northwest recreational block (Ties), short due to rain
20150806.01	Production in northwest recreational block (Ties)
20150806.02	Production in NE Corner block (Ties)
20150806.03	Production in NE Corner block, short due to rain
20150807.01	Production in NE Corner block
20150807.02	Production in NE Corner block
20150808.01	Production in NE Corner block
20150808.02	Production in NE Corner block
20150808.03	Production in northwest recreational block. Area completed
20150809.01	Production in middle of Peace block
20150809.02	Production in middle of Peace block
20150809.03	Production in middle of Peace block
20150810.01	Production in middle of Peace block
20150810.02	Production in middle of Peace block
20150810.03	Production in middle of Peace block
20150810.04	Production in middle of Peace block
20150810.05	Production in middle of Peace block
20150811.01	Production in middle of Peace block
20150811.02	Production in middle of Peace block
20150811.03	Production in middle of Peace block
20150811.04	Production in middle of Peace block
20150812.01	Production in middle of Peace block
20150812.02	Production in middle of Peace block
20150812.03	Production in middle of Peace block
20150812.04	Production in middle of Peace block and ties
20150812.05	Production in middle of Peace block and ties.
20150813.01	Production in middle of Peace block and ties
20150813.02	Production in middle of Peace block and ties
20150813.03	Production in middle of Peace block and ties
20150813.04	Production in middle of Peace block and ties
20150813.05	HA Test
20150814.01	Production in middle of Peace block and ties
20150814.02	Production in middle of Peace block and ties
20150814.03	Production in middle of Peace block and ties
20150814.04	Production in middle of Peace block and ties
20150814.05	Production in middle of Peace block and ties
20150815.01	Production in Peace block southwest zone
20150815.02	Production in Peace block southwest zone and HFRN Infill
20150815.03	Production in Peace block southwest zone,
20150816.01	Production in Peace block southwest zone
20150816.02	Production in Peace block southwest zone
20150816.03	Production in Peace block southwest zone, remobilisation to S1
20150817.01	Production in Peace block southwest zone

20150817.02	Production in Peace block southwest zone, cut short due to weather.
20150817.03	Production in Peace block southwest zone
20150818.01	Production in Peace block southwest zone
20150818.02	Production in Peace block southwest zone
20150818.03	Production in Peace block southwest zone
20150818.04	Production in Peace block southwest zone
20150819.01	Aborted flight due to frame back left joint looking high during takeoff
20150819.02	Production in Peace block southwest zone
20150819.03	Production in Peace block southwest zone
20150819.04	Production in Peace block southwest zone
20150819.05	Production in Peace block southwest zone
20150820.01	Production in Peace block southwest zone
20150820.02	Production in Peace block southwest zone
20150821.01	Production in the Doig block
20150821.02	Production in the Doig block
20150821.03	Production in the Doig block
20150821.04	Production in the Peace block
20150822.01	Production in the Charlie Lake block
20150822.02	Production in the Charlie Lake block

Appendix 6: Digital data

The digital data are listed in the following folders.

Data delivery folder	Sub folder	Sub folder	File format	Comment
01_Data	01_GDB		Geosoft.gdb	EM and MAG database ready for import in Geosoft
02_Inversion	01_GDB_Models		Geosoft.gdb	Database file containing EM inversion results, ready for import in Geosoft
	02_Layer_ Resistivity_Grids	01_GS_grd 02_GeoTiff	Geosoft.grd .tif	Grids of the resistivity in each layer
	03_Layer_ Resistivity_Maps	01_GS_maps 02_Pdf	.map .pdf	Maps and pdf's of the resistivty in each layer
	04_Sections	01_Png	.png	Layer mean resistivity and analysis of all lines
03_Maps	01_DEM	01_GS_maps 02_Pdf	.map .pdf	Maps and PDF of DEM
	02_Linepath	01_GS_maps 02_Pdf	.map .pdf	Maps and PDF of Flown Lines
	03_Planned FlightLines	01_GS_maps 02_Pdf	.map .pdf	Maps and PDF of Planned Flight Lines
	04_MAG	01_GS_maps 02_Pdf	.map .pdf	Maps and PDF's of Magnetic data
	05_PLNI	01_Png 02_Pdf	.png .pdf	Power Line Noise Indicator
04_Grids	01_DEM		Geosoft.grd	Digital Elevation Model (DEM) in Geosoft grd.
	02_EM	HM_Z	Geosoft.grd	Height corrected channel plots of raw data. Gate 11-37
		LM_Z	Geosoft.grd	Height corrected channel plots of raw data. Gate 9-28
	03_MAG		Geosoft.grd	Geosoft grd grids of Magnetic data
	04_PLNI		Geosoft.grd	Geosoft grd of PLNI
05_Report			.pdf	The report and appendices

Subfolders containing the Peace block (incl. the north-eastern corner and the infill lines HRFN), the DOIG block and the Charlie Lake block have been made in each directory.